

Top couplings

Jahred Adelman,
Department of Physics, Yale University, New Haven, CT 06511

Barbara Alvarez Gonzalez,
Department of Physics and Astronomy, Michigan State University, East Lansing MI 48824

Yang Bai,
Department of Physics, University of Wisconsin, Madison, WI 53706

Matthew Baumgart,
Department of Physics, Carnegie Mellon University, Pittsburgh, PA 15213

R. Keith Ellis,
Theoretical Physics Department, Fermilab, Batavia, IL 60510

A. Khanov,
Department of Physics, Oklahoma State University, Stillwater OK 74078

Andrey Loginov,
Department of Physics, Yale University, New Haven, CT 06511

Marcel Vos,
IFIC (UVEG/CSIC), Ap. Correos 22085, E46071 Valencia, Spain

ABSTRACT: Overview on top couplings measurements is presented, and the prospects of future measurements are discussed. The coupling of top to the W boson can be examined either by looking at the decay of the top quark or from single top quark production. With the advent of high statistics top physics at the LHC and at the high-luminosity LHC, the processes where the bosons (photon, Z and Higgs) are produced in association with top quarks become accessible. The first evidence on the coupling of the top quark to these particles will come from the production rate.

KEYWORDS: QCD, Phenomenological Models, Hadronic Colliders, LHC

Contents

1	Standard Model couplings¹	2
1.1	Top + γ	2
1.2	Top + Z	3
1.3	Top + H	3
1.4	Top + W	4
2	Theory of non-standard couplings²	5
2.1	General considerations	5
2.2	tW couplings	5
2.3	tZ , $t\gamma$ and tg couplings	6
2.4	tH couplings	7
2.5	Top Quark Couplings to Dark Matter	7
2.6	Constraints on non-standard couplings	7
3	Top Quark Weak Interaction Measurements³	8
3.1	t -channel single top production	9
3.2	Wt -channel single top production	10
3.3	s -channel single top production	11
4	Coupling of the Top quark to charge zero vector bosons⁴	11
4.1	Introduction	11
4.2	$t\bar{t}\gamma$	11
4.3	$t\bar{t}Z$	13
4.4	Linear Collider prospects ⁵	14
5	Coupling of the Top quark to the Higgs boson⁶	17
5.1	Searches for $t\bar{t} + H$	17
6	Top quark + jets⁷	19
6.1	$t\bar{t}$ with central jet veto	19
6.2	Jet multiplicity in $t\bar{t}$ events and $t\bar{t}$ +jet production cross section	20
6.3	$t\bar{t}$ +jets heavy flavor composition	20

¹Author: R. Keith Ellis, Fermilab

²Authors: Yang Bai, University of Wisconsin and Matthew Baumgart, Carnegie Mellon

³Author: Barbara Alvarez Gonzalez, Michigan State University

⁴Author: Andrey Loginov, Yale University

⁵Author: Marcel Vos, IFIC (UVEG/CSIC)

⁶Author: Jahred Adelman, Yale University

⁷Author: Sasha Khanov, OK State University

1 Standard Model couplings¹

The top quark couples to other Standard Model fields through its gauge and Yukawa interactions. At LHC energies the top quark is copiously produced both in pair production and in the three single top processes mediated by the exchange or production of a W -boson. Fig. 1 shows the cross sections for these processes as a function of the centre of mass energy.

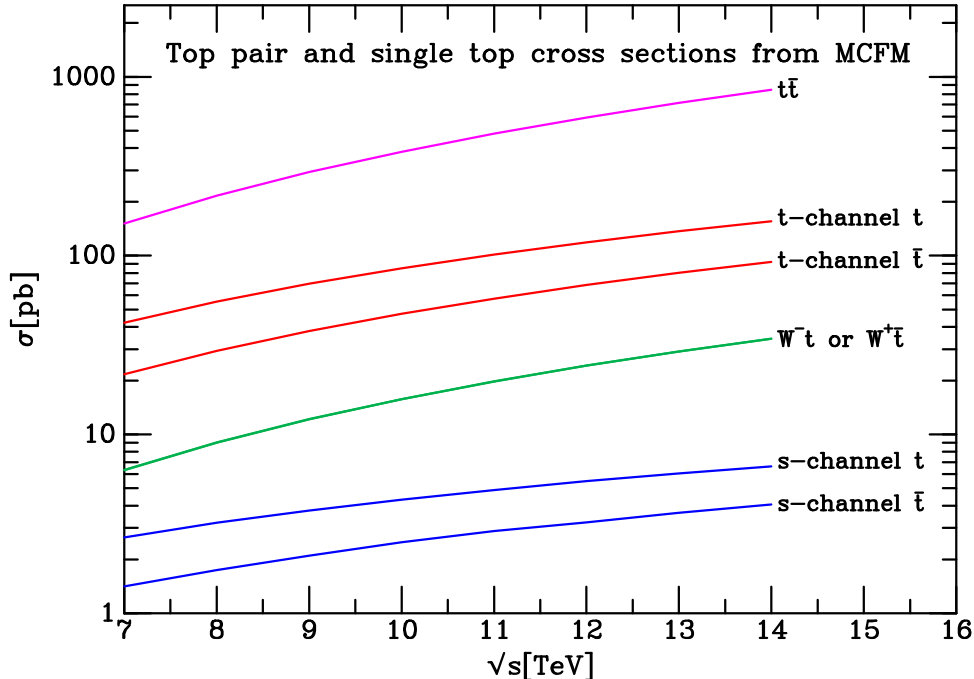


Figure 1. NLO values for the top cross sections vs \sqrt{s} calculated using MCFM. The cross sections are evaluated at factorization and renormalization scale $m_t = 173.2$ GeV using the CTEQ6M parton distributions.

With the advent of high statistics top physics at the LHC, the processes where the bosons, γ, Z and H are produced in association with top quarks become accessible. The first evidence on the coupling of the top quark to these particles will come from the production rate. The coupling of top to the W boson can be examined either by looking at the decay of the top quark or from single top quark production. Two recent reviews of the experimental situation for top couplings can be found in ref. [1, 2].

1.1 Top + γ

Experimental results on the production of a photon in association with a top pair have been presented by both the CDF collaboration[3] and the ATLAS collaboration[4]. Next-to-leading order (NLO) corrections to the top cross section in association with a photon are given in refs. [5, 6]. When confronting theory with experimental data it is important to include photon radiation off top quark decay products, which are found to give a significant contribution to the cross-section [5].

¹Author: R. Keith Ellis, Fermilab

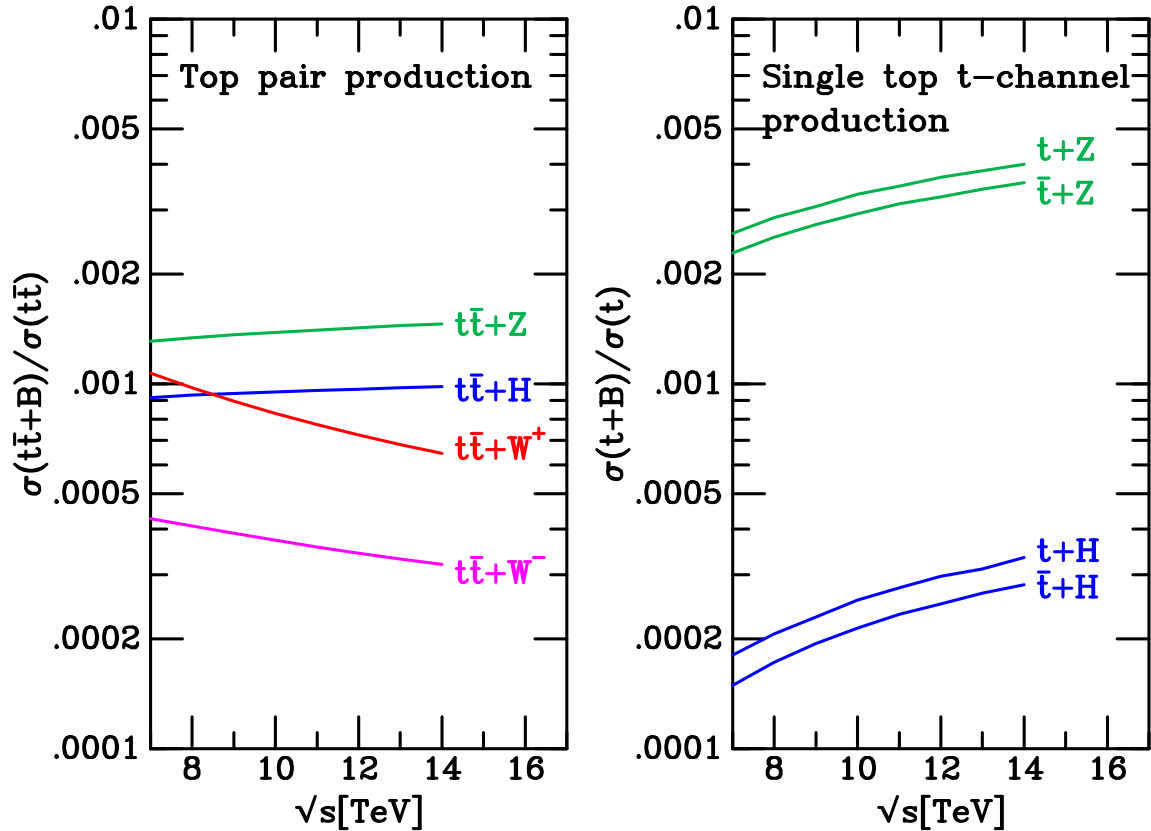


Figure 2. Fraction of top pair (left pane) and t-channel single-top production which is accompanied by a massive boson. The $t\bar{t} + W^\pm$ process is included for completeness, even though the W does not couple to the top quark. The ratios are calculated in lowest order perturbation theory.

1.2 Top + Z

The primary source of information on the coupling of the top to the Z -boson will come from the associated production of the Z with a top quark. A first measurement of vector boson production in association with top-antitop pairs is given in ref. [7]. A search for this final state has also been performed by ATLAS [8]. Flavor changing couplings of the top quark to the Z are limited by the limits on neutral current decay of the top quark [9, 10].

Also of interest is the associated production of a Z -boson in single top production, since it is sensitive to the couplings of the Z to both the W -boson and the quarks, including the top. Fig. 2 shows the production of $t\bar{t} + Z$ and the production of $t + Z$ and $\bar{t} + Z$ as a fraction of the corresponding cross section without a vector boson. At $\sqrt{s} = 14$ TeV the $t\bar{t}$ pair cross section is about 1 nb and the single top production cross section for t (\bar{t}) is about 150(100) pb.

1.3 Top + H

Indirect evidence of the coupling of the top to the Higgs boson comes from the Higgs boson production rate in pp collisions at the LHC. The gluon-gluon fusion production of the Higgs boson is predicted to

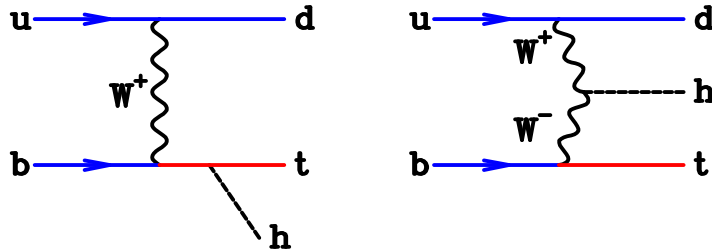


Figure 3. Diagrams for the production of the Higgs in association with a single top.

proceed predominantly through a top loop. The decay of the Higgs, $H \rightarrow \gamma\gamma$ also proceeds through a top loop (and a W -boson) loop and will provide complementary information.

Further information will have to await the observation of the direct production process, $t\bar{t} + H$. Fig. 2 shows the production of $t\bar{t} + H$ and the production of $t + H$ and $\bar{t} + H$ as a fraction of the cross section without the corresponding vector boson. Theoretical predictions for $t\bar{t}H$ production at next-to-leading order can be found in refs. [11–15].

The production of the Higgs in association with a single top is of interest because of the substantial cancellation between the two diagrams where the Higgs is emitted from the top quark or from the W -boson exchanged in the t -channel, as shown in Fig. 3. After inclusion of the branching ratios the cross section is very small, perhaps beyond the limit of observability at the high luminosity LHC. Thus any non-standard physics that affects the cancellation such as a change of sign of the coupling to the top will lead to a much larger cross section. For a discussion of this process and references to recent literature, see refs. [16–20].

1.4 Top + W

Constraints on the couplings of the top to the W come from top decay and from single top production. Measurements of the W boson helicity in top decay probes the structure of the Wtb vertex. In the standard model the branching fraction of the top quark to longitudinal W bosons is given by,

$$\frac{\Gamma(t \rightarrow bW_0)}{\Gamma(t \rightarrow bW)} = F_0 = \frac{m_t^2}{m_t^2 + 2M_w^2} \quad (1.1)$$

where we have neglected the mass of the b quark. The polarization state of the W controls the angular distribution of the leptons into which it decays. We may define the lepton helicity angle θ_e^* , as the angle of the charged lepton in the rest frame of the W , with respect to the original direction of travel of the W . The normalized angular distribution of the charged leptons is therefore given by,

$$\frac{1}{N} \frac{dN(W \rightarrow e\nu)}{d \cos \theta_e^*} = \left[\frac{3}{4} \sin^2 \theta_e^* F_0 + \frac{3}{8} (1 - \cos \theta_e^*)^2 F_L + \frac{3}{8} (1 + \cos \theta_e^*)^2 F_R \right], \quad (1.2)$$

where $F_0 + F_L + F_R = 0$. Recent measurements of the W -boson helicity fraction have been presented by CDF [21], D0 [22], CMS [23] and ATLAS [24] and CDF and D0 combined [25].

Data on single top production also constrains the form of the Wtb vertex [26, 27]. The majority of the data has so far been used to constrain the normalization and to place a constraint on the CKM mixing and V_{tb} [28].

2 Theory of non-standard couplings²

2.1 General considerations

The effects of new physics at a high scale $\Lambda \gg v \equiv 246$ GeV can be described by an effective Lagrangian,

$$\mathcal{L}^{\text{eff}} = \sum \frac{C_i}{\Lambda^2} \mathcal{O}_i + \dots, \quad (2.1)$$

where the \mathcal{O}_i are higher dimension operators. The leading contributions enter at dimension six. They include corrections to $t\bar{t}V$ gauge vertices, four-fermion operators, and couplings involving gluons that will appear in $t\bar{t}$ production. The vertex function approach [29–32] can be mapped into the operator method as we discuss in Section 2.2. The latter has the advantage of generality and can be used with off-shell particles and in loop calculations. Since the prefactor for our dimension six operators involving the Higgs is v^2/Λ^2 or $(m_t v/\Lambda^2)$ instead of E^2/Λ^2 , many of these do not decouple at low energies. This is an experimental boon as it allows us to probe new physics in the top sector with low energy experiments, as we describe in Section 2.6. The top couplings often enter the relevant observables at loop level, and thus effective field theory is the theoretically consistent description.

Ref. [33] reduces an overcomplete basis of operators using equations of motion and gauge invariance. However, only processes affecting the top quark’s interaction with gauge bosons were considered. Additional modifications of single and doubly produced tops from four-fermion operators are given in [34]. Its authors mainly consider $t\bar{t}$ produced in the color octet state as only this will interfere with the SM. Also given in [34] are higher dimension operators without tops that nonetheless affect $t\bar{t}$ production. To this we add our own list of operators relevant for tt (distinct from $t\bar{t}$) processes, which could also contribute to color singlet $t\bar{t}$.

2.2 tW couplings

The first four operators can affect the Wtb couplings. To match the traditional formulas in terms of form factors defined as

$$\mathcal{L}_{\text{int}} \supset -\frac{g}{\sqrt{2}} \bar{b} \gamma^\mu (c_L^W P_L + c_R^W P_R) t W_\mu^- - \frac{g}{\sqrt{2}} \bar{b} \frac{i\sigma^{\mu\nu} q_\nu}{M_W} (d_L^W P_L + d_R^W P_R) t W_\mu^- + h.c., \quad (2.2)$$

where q is the W momentum and c_L^W equals the CKM matrix element $V_{tb} \approx 1$ and c_R^W, d_L^W, d_R^W vanish at the tree level in the SM. We have the modifications of these form factors from the four dimension-six operators [33]:

$$\delta c_L^W = C_{\phi q}^{(3)*} \frac{v^2}{\Lambda^2}, \quad \delta d_L^W = \sqrt{2} C_{dW} \frac{v^2}{\Lambda^2}, \quad (2.3)$$

$$\delta c_R^W = \frac{1}{2} C_{\phi\phi}^{(3)*} \frac{v^2}{\Lambda^2}, \quad \delta d_R^W = \sqrt{2} C_{uW} \frac{v^2}{\Lambda^2}. \quad (2.4)$$

In principle, the form factors should be functions of the momentum q . The additional q^2 terms in the form factors will match to higher-dimensional operators (*e.g.* dimension-8 operators). Since there are two expansion parameters, v^2/Λ^2 and q^2/Λ^2 , to use the effective operators, one needs to be cautious and should not have the momentum in the process to be above Λ as stressed in [30]. Existing collider studies on probing anomalous Wtb couplings in single top production can be found in [29].

²Authors: Yang Bai, University of Wisconsin and Matthew Baumgart, Carnegie Mellon

Table 1. Dimension-6 operators for $t\bar{t}$ production, single t production, t decay, and tt production. The q and u fields without flavor superscript are third generation, except for the neutral current and tt sections where i and j run from 1-3. As usual, $\tilde{\phi} = \epsilon\phi^*$.

Charged current single top production and top decay	
$\mathcal{O}_{\phi q}^{(3)} = i(\phi^\dagger \tau^I D_\mu \phi)(\bar{q}\gamma^\mu \tau^I q)$	$\mathcal{O}_{\phi\phi} = i(\tilde{\phi}^\dagger D_\mu \phi)(\bar{u}\gamma^\mu d)$
$\mathcal{O}_{uW} = (\bar{q}\tau^I \sigma^{\mu\nu} u)\phi W_{\mu\nu}^I$	$\mathcal{O}_{dW} = (\bar{q}\tau^I \sigma^{\mu\nu} d)\phi W_{\mu\nu}^I$
Neutral current top production and top decay	
$\mathcal{O}_{\phi q}^{(1)} = i(\phi^\dagger D_\mu \phi)(\bar{q}^i \gamma^\mu q^j)$	$\mathcal{O}_{\phi u} = i(\phi^\dagger D_\mu \phi)(\bar{u}^i \gamma^\mu u^j)$
$\mathcal{O}_{uB} = (\bar{q}^i \sigma^{\mu\nu} u^j)\phi B_{\mu\nu}$	
Single top and $t\bar{t}$ production	
$\mathcal{O}_{uG} = (\bar{q}\lambda^a \sigma^{\mu\nu} u)\tilde{\phi} G_{\mu\nu}^a$	$\mathcal{O}_{qq}^{(1,3)} = (\bar{q}^i \gamma_\mu \tau^I q^j)(\bar{q}\gamma^\mu \tau^I q)$
$t\bar{t}$ production	
$\mathcal{O}_{qq}^{(8,1)} = (\bar{q}^i \gamma_\mu \lambda^a q^j)(\bar{q}\gamma^\mu \lambda^a q)$	$\mathcal{O}_{qq}^{(8,3)} = (\bar{q}^i \gamma_\mu \lambda^a \tau^I q^j)(\bar{q}\gamma^\mu \lambda^a \tau^I q)$
$\mathcal{O}_{ut}^{(8)} = (\bar{u}^i \gamma_\mu \lambda^a u^j)(\bar{u}\gamma^\mu \lambda^a u)$	$\mathcal{O}_{dt}^{(8)} = (\bar{d}^i \gamma_\mu \lambda^a d^j)(\bar{u}\gamma^\mu \lambda^a u)$
$\mathcal{O}_{quS}^{(1)} = (\bar{q}u^i)(\bar{u}^j q)$	$\mathcal{O}_{qdS}^{(1)} = (\bar{q}d^i)(\bar{d}^j q)$
$\mathcal{O}_{qtS}^{(1)} = (\bar{q}u)(\bar{u}q)$	
Gluon operators that affect $t\bar{t}$ production	
$\mathcal{O}_G = f_{ABC} G_\mu^{A\nu} G_\nu^{B\rho} G_\rho^{C\mu}$	$\mathcal{O}_{\tilde{G}} = f_{ABC} \tilde{G}_\mu^{A\nu} G_\nu^{B\rho} G_\rho^{C\mu}$
$\mathcal{O}_{\phi G} = \phi^\dagger \phi G_{\mu\nu}^A G^{A\mu\nu}$	$\mathcal{O}_{\phi\tilde{G}} = \phi^\dagger \phi \tilde{G}_{\mu\nu}^A G^{A\mu\nu}$
$\mathcal{O}_{GB} = G_\mu^{A\nu} G_\nu^{A\rho} B_\rho^{C\mu}$	
tt production and color singlet $t\bar{t}$ production	
$\mathcal{O}_{qqV}^{(1)} = (\bar{q}^i \gamma_\mu q^j)(\bar{q}^k \gamma^\mu q^l)$	$\mathcal{O}_{qq}^{(3)} = (\bar{q}^i \gamma_\mu \tau^I q^j)(\bar{q}^k \gamma^\mu \tau^I q^l)$
$\mathcal{O}_{quV}^{(1)} = (\bar{q}^i \gamma_\mu q^j)(\bar{u}^k \gamma^\mu u^l)$	$\mathcal{O}_{uuV}^{(1)} = (\bar{u}^i \gamma_\mu u^j)(\bar{u}^k \gamma^\mu u^l)$
$t\bar{t}h$ coupling	
$\mathcal{O}_{3\phi} = \phi^\dagger \phi \phi \bar{q} u$	

2.3 tZ , $t\gamma$ and tg couplings

The $t\bar{t}Z$ couplings are similar to those involving the W . The vertices take the form

$$\mathcal{L}_{int} \supset -\frac{g}{2c_W} \bar{t} \gamma^\mu (c_L^Z P_L + c_R^Z P_R - 2s_W^2 Q_t) t Z_\mu - \frac{g}{2c_W} \bar{t} \frac{i\sigma^{\mu\nu} q_\nu}{M_Z} (d_V^Z + id_A^Z \gamma_5) t Z_\mu, \quad (2.5)$$

with $Q_t = 2/3$ as the electric charge of the top quark and $c_W = \cos\theta_W$. In the SM, the couplings are $c_L^Z = 1$, $c_R^Z = 0$ and $d_{V,A}^Z = 0$ at the tree level. The match to the dimension-six operators is given by

$$\delta c_L^Z = \text{Re} \left[C_{\phi q}^{(3)} - C_{\phi q}^{(1)} \right] \frac{v^2}{\Lambda^2}, \quad \delta d_V^Z = \sqrt{2} \text{Re} [c_W C_{uW} - s_W C_{uB}] \frac{v^2}{\Lambda^2}, \quad (2.6)$$

$$\delta c_R^Z = -\text{Re} [C_{\phi u}] \frac{v^2}{\Lambda^2}, \quad \delta d_R^W = \sqrt{2} \text{Im} [c_W C_{uW} - s_W C_{uB}] \frac{v^2}{\Lambda^2}. \quad (2.7)$$

For the $t\bar{t}\gamma$ couplings, the vertices are

$$\mathcal{L}_{int} \supset -e Q_t \bar{t} \gamma^\mu t A_\mu - e \bar{t} \frac{i\sigma^{\mu\nu} q_\nu}{m_t} (d_V^\gamma + id_A^\gamma \gamma_5) t A_\mu. \quad (2.8)$$

Here, the couplings d_V^γ and d_A^γ are related to the top quark magnetic and electric dipole moment, respectively. The match to the dimension-six operators is given by

$$\delta d_V^\gamma = \frac{\sqrt{2}}{e} \text{Re} [c_W C_{uB} + s_W C_{uW}] \frac{v m_t}{\Lambda^2}, \quad \delta d_A^\gamma = \frac{\sqrt{2}}{e} \text{Im} [c_W C_{uB} + s_W C_{uW}] \frac{v m_t}{\Lambda^2}. \quad (2.9)$$

To measure the $t\bar{t}\gamma$ couplings, it is important to know the SM next-to-leading order QCD corrections [5].

For the $t\bar{t}g$ couplings, the vertices are

$$\mathcal{L}_{int} \supset -g_s \bar{t} \frac{\lambda^a}{2} \gamma^\mu t G_\mu^a - g_s \bar{t} \gamma^a \frac{i\sigma^{\mu\nu} q_\nu}{m_t} (d_V^g + i d_A^g \gamma_5) t G_\mu^a. \quad (2.10)$$

Here, the couplings d_V^g and d_A^g are related to the top quark chromo-magnetic and chromo-electric dipole moment, respectively. The match to the dimension-six operators is given by

$$\delta d_V^g = \frac{\sqrt{2}}{g_s} \text{Re} [C_{uG}] \frac{v m_t}{\Lambda^2}, \quad \delta d_A^g = \frac{\sqrt{2}}{g_s} \text{Im} [C_{uG}] \frac{v m_t}{\Lambda^2}. \quad (2.11)$$

2.4 tH couplings

The $t\bar{t}h$ vertex is given by

$$\mathcal{L}_{int} \supset -\frac{\sqrt{2} m_t}{v} c_t^h h \bar{t} t - c_t^{h5} h \bar{t} i \gamma_5 t. \quad (2.12)$$

In the SM, $c_t^h = 1$ and $c_t^{h5} = 0$. With the new physics from dimension-six operators, we have

$$\delta c_t^h = -\frac{3}{\sqrt{2}} \text{Re} C_{3\phi} \frac{v^2}{\Lambda^2}, \quad \delta c_t^{h5} = \left(\text{Im} C_{\phi q}^{(3)} - \text{Im} C_{\phi q}^{(1)} + \text{Im} C_{\phi u}^{(1)} \right) \frac{v m_t}{\Lambda^2}. \quad (2.13)$$

Additional interactions like $t\bar{t}hg$ can be generated by the \mathcal{O}_{uG} operator and will affect the $t\bar{t} + h$ production cross sections. Collider studies on measuring the top Yukawa coupling at the ILC at $\sqrt{s} = 500$ GeV can be found in [35]. Associated production of Higgs and single top at hadron colliders can be found in [16, 17].

2.5 Top Quark Couplings to Dark Matter

Assuming dark matter is a weak scale particle, we can make a list of effective operators for the top quark couplings to χ . For a Dirac fermion χ , we have [36]

$$\mathcal{L}_{int} \supset \frac{1}{\Lambda_1^2} \bar{\chi} \chi \bar{t} t + \frac{1}{\Lambda_2^2} \bar{\chi} \gamma_5 \chi \bar{t} \gamma_5 t + \frac{1}{\Lambda_3^2} \bar{\chi} \gamma^\mu \chi \bar{t} \gamma_\mu t + \frac{1}{\Lambda_4^2} \bar{\chi} \gamma_\mu \gamma_5 \chi \bar{t} \gamma^\mu \gamma_5 t + h.c.. \quad (2.14)$$

The signal could be $t\bar{t} + \text{MET}$. One can also close the top quark loop and discuss mono-jet + MET at a hadron collider [37] and/or mono-photon + MET at a linear collider.

2.6 Constraints on non-standard couplings

Several papers have placed constraints on either the coefficients of the operators in Table 1 and/or the couplings in Sections 2.2-2.4. In general, the limits are placed on couplings that affect $t\bar{t}V$ and Wtb vertices. In some cases, the limits involve actual data, in others they are hypothetical, invoking either future LHC data or the ILC. In [38] and [39], the authors follow up on the basis written down in [34]. Along with the helicity fraction in top decays, they use precision electroweak data and results from

$\bar{B} \rightarrow X_s \gamma$ and $B - \bar{B}$ mixing to constrain the nine dimension-6 operators that couple 3rd generation quarks to electroweak bosons, a list that strongly overlaps with Table 1. B -physics observables are also used to place limits on Wtb couplings in [40]. Refs. [30, 41] discuss possible bounds on Wtb at the LHC. In [31, 32], future LHC data is simulated along with the ILC for constraining top couplings to vector bosons. In [42], the operator basis is discussed in the context of the ILC along with the claim that beam polarization and a CM energy of 1 TeV would allow one to separately probe all the operators contributing to $t\bar{t}Z$ and $t\bar{t}\gamma$ couplings. Lastly, by using alternative W helicity variables, ref. [43] proposes to measure phases in the Wtb couplings that are otherwise difficult to access.

In addition to discussing electroweak couplings, [44] uses Tevatron and LHC data on the overall $t\bar{t}$ cross section to constrain the top’s chromomagnetic and electric dipole moments (respectively given by the real and imaginary coefficients of \mathcal{O}_{uG}). In addition to collider data, [45] uses neutron and mercury EDMs along with B decays to place limits on the top’s chromo and regular dipole moments. Ref. [46] uses top quark spin correlations in a complementary approach to constrain the top’s color dipole moments. For those operators involving neutral currents, ref. [47] uses CDF and ZEUS data to place constraints on $t \rightarrow Zq$ and $t \rightarrow \gamma q$ decays. Also, [48] discusses the potential reach of the LHC to study FCNC top decays. As more LHC data becomes available, one can constrain more of the operators in Table 1. The overall $t\bar{t}$ rate will place limits on the “ $t\bar{t}$ production” set, including many four quark operators that have yet to be significantly bounded. Additionally, $t\bar{t}$ or 4 top (*cf.* [49]) events could give additional information on the four fermion subset of Table 1. Lastly, the direct observation of $t\bar{t}h$ events will allow us to better determine the coefficients of the many operators that couple tops and Higgses.

3 Top Quark Weak Interaction Measurements³

This section presents a summary of the current studies on the single top-quark production at the LHC and the Tevatron. There are multiple processes that can lead to the production of a top-quark. The dominant mechanism for creating top-quarks at hadron colliders is the production of a top-antitop pair through QCD interactions. The top-quark can also be produced singly by an electroweak Wtb -vertex with a smaller cross-section than for top-antitop production. The SM single top-quark production proceeds through three different mechanisms shown in Fig. 4: t -channel exchange of a W -boson, associated production of a top-quark and a W boson (Wt -channel), and s -channel production and decay of a virtual W boson. The theoretical cross-section predictions for these processes at different center-of-mass energies are given in Table 2.

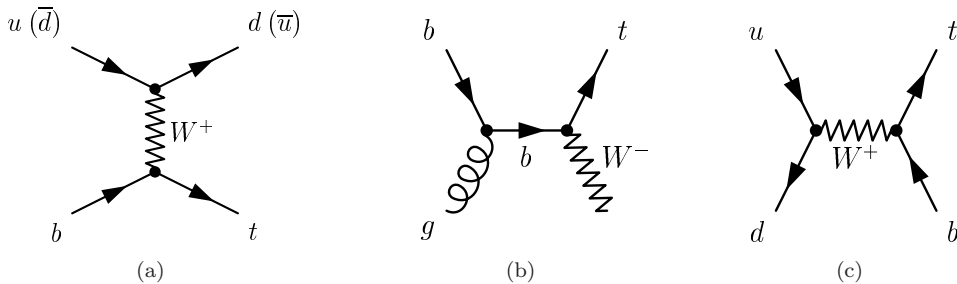


Figure 4. Feynman diagrams of single top-quark production processes.

³Author: Barbara Alvarez Gonzalez, Michigan State University

E_{CM} [TeV]	t -channel	Wt -channel	s -channel
1.96	2.10 ± 0.19 pb	0.22 ± 0.08 pb	1.05 ± 0.07 pb
7	$64.57^{+3.32}_{-2.62}$ pb	$15.74^{+1.34}_{-1.36}$ pb	$4.63^{+0.29}_{-0.27}$ pb
8	87.8 ± 3.4 pb	22.4 ± 1.5 pb	5.6 ± 0.3 pb

Table 2. Approximate next-to-next-to-next-to-leading (NNNLO) and next-to-next-to-leading (NNLO) single top-quark production cross-sections at different center-of-mass energies [50–53] with $m_{top}=172.5$ GeV/ c^2 . The Tevatron (1.96 TeV) cross sections are calculated at approximate NNNLO. The LHC (7 and 8 TeV) cross sections are calculated at approximate NNLO.

There are several motivations to study single top production: single top production gives complementary information on top-quark properties, it allows a direct measurement of the CKM matrix element V_{tb} , and is sensitive to many models of new physics. Furthermore, determining the cross-section also allows to extract the b -quark density.

This section is organized as follows: t -channel and Wt -channel production cross-section measurements including the determination of V_{tb} are presented, followed by a review of searches in the tb final states such as s -channel and W' .

3.1 t -channel single top production

The t -channel single top production is dominant both at the Tevatron and at the LHC. The measurements of the t -channel single top-quark production cross-section with the ATLAS detector are done using a neural network based discriminant. Selected events in the lepton+jets channel contain one lepton, missing transverse momentum, and two or three jets, including one which is b -tagged. The t -channel production cross-section is measured by performing a combined binned maximum likelihood fit to the neural network output distribution for the observed data resulting in $\sigma_t=95 \pm 18$ pb with 5.8 fb $^{-1}$ at 8 TeV [54] and $\sigma_t=83 \pm 4(\text{stat})^{+20}_{-19}(\text{syst})$ pb using 1.04 fb $^{-1}$ at 7 TeV [55], which are in good agreement with the SM prediction. Major systematic uncertainties considered include jet energy scale (JES), b -tagging efficiency, and the amount of initial- and final-state radiation. Using the ratio of the measured to the predicted cross-section and assuming that the top-quark-related CKM matrix elements obey the relation $|V_{tb}| \gg |V_{ts}|, |V_{td}|$, the coupling strength at the $W-t-b$ vertex is determined to be $|V_{tb}|=1.04^{+0.10}_{-0.11}$ at 8 TeV and $|V_{tb}| = 1.13^{+0.14}_{-0.13}$ at 7 TeV. If it is assumed that $|V_{tb}| \leq 1$, a lower limit of $|V_{tb}| > 0.80$ (0.75) at 8 (7) TeV is obtained at 95% CL. With the same selection described above and the same analysis technique the top-quark and top-antiquark production cross-sections are also measured using an integrated luminosity of 4.7 fb $^{-1}$ at 7 TeV. A binned maximum likelihood fit to the output distribution of neural networks that are split according to the charge of the lepton is performed resulting in $\sigma_t(t)=53.2 \pm 10.8$ pb and $\sigma_t(\bar{t})=29.5^{+7.4}_{-7.5}$ pb [56]. A cross-section ratio of $R_t=1.81^{+0.23}_{-0.22}$ is measured. At the current precision, the measurement is in agreement with the predictions based on various global PDF sets that range from 1.86 to 2.07.

The CMS strategies for the t -channel single top cross-section analyses at 7 and 8 TeV are different. The 8 TeV result uses only the leptonic decay channel with a muon in the final state. The pseudorapidity distribution of the recoil jet is exploited for the measurement. With an integrated luminosity of 5.0 fb $^{-1}$ the cross-section is found to be $80.1 \pm 5.7(\text{stat}) \pm 11.0(\text{syst}) \pm 4.0(\text{lumi})$ pb [57]. The largest systematic uncertainties are from statistical uncertainty, JES and t -channel generator uncertainties. $|V_{tb}|$ is also measured at the 10% level obtaining a lower bound of $|V_{tb}| > 0.81$ at 95% CL. The CMS results at 7 TeV followed two different and complementary approaches. The first approach exploits the distributions of the pseudorapidity of the recoil jet and reconstructed top-quark mass. The second ap-

proach is based on multivariate analysis techniques. In this case, both the muon and the electron decay channels have been used, corresponding to integrated luminosities of 1.17 and 1.56 fb⁻¹, respectively. The single top-quark production cross-section in the t -channel is measured to be 67.2±6.1 pb [58]. The largest systematic uncertainties are from statistical uncertainty, W+jets normalization and generator uncertainties. A lower limit of $|V_{tb}| > 0.92$ is obtained at 95% CL using the SM assumption of $|V_{tb}| < 1$.

Following the first observation of single top-quark production in 2009 at the Tevatron [59–61], both collaborations, CDF and D0, have updated their single top results. D0 presents measurements of production cross sections of single top-quarks in $p\bar{p}$ collisions at 1.96 TeV in a data sample corresponding to an integrated luminosity of 5.4 fb⁻¹. Selected events with an isolated electron or muon, an imbalance in transverse energy, and two, three, or four jets, with one or two of them containing a b -quark. Three different multivariate analysis techniques to extract the signal are used in this analysis. The measured inclusive cross section, for t -channel and s -channel together, is $\sigma=3.43_{-0.74}^{+0.73}$ pb and it is used to extract the CKM matrix element $0.79 < |V_{tb}| \leq 1$ at the 95% CL. The largest uncertainties arise from the JES, JER, corrections to b -tagging efficiencies, and the correction for jet-flavor composition in W+jets events. The cross sections are also measured separately to be $\sigma_s=0.68_{-0.35}^{+0.38}$ pb and $\sigma_t=2.86_{-0.63}^{+0.69}$ pb [62], assuming, respectively, t -channel and s -channel production rates as predicted by the SM.

A measurement of single top-quark production in lepton+jets final state using 7.5 fb⁻¹ of data collected by CDF Run II experiment is also presented. Selected events contain a charged lepton, electron or muon, missing transverse energy and two or three jets, at least one of them b -tagged. A Neural Network multivariate method is used to discriminate signal against comparatively large backgrounds. The measured inclusive cross-section is $3.04_{-0.53}^{+0.57}$ pb (stat+syst) [63] and the CKM matrix element value $V_{tb}=0.96\pm 0.09(\text{stat+syst})\pm 0.05(\text{theory})$ with a lower limit of $|V_{tb}| > 0.78$ at the 95% CL. The systematic uncertainty source with the biggest contribution is the background normalization. The s -channel and t -channel cross sections are also extracted separately performing a two dimensional fit, $\sigma_s=1.81_{-0.58}^{+0.63}$ pb and $\sigma_t=1.49_{-0.42}^{+0.47}$ pb.

3.2 Wt -channel single top production

The Wt -channel is negligible at the Tevatron but it has the second highest cross-section among single top processes at the LHC. The CMS and ATLAS collaborations have shown evidence for the associated production of a W boson and a top-quark. The CMS measurement is performed using events with two leptons and a jet originating from a b -quark. A multivariate analysis based on kinematic properties is exploited to separate the main background contribution, $t\bar{t}$, from the signal. The observed signal has a significance of 4.0σ and corresponds to a cross-section of 16_{-4}^{+5} pb [64] with 4.9 fb⁻¹ at 7 TeV. The measurement can be used to determine the absolute value of the CKM matrix element $|V_{tb}| = 1.01_{-0.13}^{+0.16}(\text{exp})_{-0.04}^{+0.03}(\text{theo})$ assuming $|V_{ts}|$ and $|V_{td}|$ much smaller than $|V_{tb}|$.

The ATLAS Wt -channel analysis is based on the selection of the dileptonic final states with events featuring two isolated leptons, electron or muon, with significant transverse missing momentum and at least one jet. A template fit to a boosted decision tree output distribution is performed to determine the cross-section. The result is incompatible with the background-only hypothesis at the 3.3σ level. The corresponding cross-section is determined and found to be $\sigma_{Wt}=16.8\pm 2.9(\text{stat})\pm 4.9(\text{syst})$ pb [65] using 2.05 fb⁻¹ at 7 TeV. The CKM matrix element $|V_{tb}| = 1.03_{-0.19}^{+0.16}$ is derived assuming that the Wt -channel production through $|V_{ts}|$ and $|V_{td}|$ is small. The results based on the lepton+jets final state have been investigated however their contributions will result in a smaller sensitivity.

3.3 s -channel single top production

Searches in the $t\bar{b}$ final state are particularly interesting since the SM s -channel production mode itself has not been observed yet and the search for this process is sensitive to several models of new physics [66]. A search for s -channel top-quark production has been performed using 0.7 fb^{-1} of ATLAS data at a center-of-mass energy of 7 TeV. Selected events contain one lepton, missing transverse energy and two jets. The final selection requires both jets to be identified as coming from b -quarks. An observed upper limit at 95% CL on the s -channel single top-quark production cross-section of $\sigma_s < 26.5 \text{ pb}$ [67], which corresponds to about 5 times the signal SM cross-section, is obtained using a cut-based analysis.

One can also search for new heavy gauge bosons such as the W' boson by looking for $t\bar{b}$ resonances. The most stringent limits on a right-handed W'_R with SM-like couplings in the decay mode $W'_R \rightarrow t\bar{b}$ are set by the CMS experiment and excludes a W'_R boson mass below 1.85 TeV at 95% CL [68] using 5 fb^{-1} of data at 7 TeV. The $W'_R \rightarrow t\bar{b}$ decay channel has been also searched for at ATLAS [69] and at the Tevatron [70, 71].

The precision achieved in the cross-section measurements at 7 and 8 TeV is comparable with theoretical NLO and NNLO predictions. A combination of the results will provide a more precise measurements and also stronger constraints on the CKM matrix element $|V_{tb}|$. The evolution of the single top cross sections with energy are shown in Fig. 1.

4 Coupling of the Top quark to charge zero vector bosons⁴

4.1 Introduction

The top quark was discovered almost twenty years ago. However, couplings of the top quark to the neutral electroweak (EW) gauge bosons (γ and Z) have not yet been directly measured. Due to the large mass, the top quark may play a special role in EW symmetry breaking (EWSB), and therefore new physics connected with EWSB can manifest itself in top precision observables. Possible signals for new physics are deviations of the $t\bar{t}\gamma$, $t\bar{t}Z$ (and also $t\bar{b}W$) couplings from the values predicted by the Standard Model (SM).

While the associated $t\bar{t}W$ production cross section measurement is an important test of the Standard Model predictions for this low cross section process, it has little to do with the top quark (see Fig. 6). The $t\bar{b}W$ coupling has been constrained via measurements of the single top quark production cross section (see Section 3) as well as via top quark width measurements, and hence it is not covered in this Section.

The $t\bar{t}\gamma$ and $t\bar{t}Z$ couplings can not be constrained via measurements of $t\bar{t}$ production at hadron colliders via intermediate virtual γ and Z bosons, since the cross section for $pp \rightarrow t\bar{t}$ is dominated by processes involving QCD couplings. Unlike at a linear e^+e^- collider, the LHC's capability of associated $t\bar{t}\gamma$ and $t\bar{t}Z$ production has the advantage that the $t\bar{t}\gamma$ and $t\bar{t}Z$ couplings are not entangled. The $t\bar{t}\gamma$ and $t\bar{t}Z$ couplings may be measured via analysis of direct production of $t\bar{t}$ pairs in association with a γ or Z boson, respectively.

4.2 $t\bar{t}\gamma$

Radiative $t\bar{t}$ production, $t\bar{t}\gamma$, can be classified into the radiative top quark production and radiative top quark decay, as shown in Fig. 5. The coupling of the top quark to photons (and therefore the $t\bar{t}\gamma$

⁴Author: Andrey Loginov, Yale University

production cross section) is sensitive to the electric charge of the top quark. The charge of the top quark has been measured via its decay products using the track charge method (a weighted sum of the charges of tracks associated with the b -jet) and the soft lepton method (charge of the muon produced in the semi-leptonic decay $b \rightarrow \mu\nu + X$ is defined by the b -quark charge) at both the Tevatron and LHC. The $t\bar{t}\gamma$ can also yield constraints to excited top quarks ($t \rightarrow t^*\gamma$) production. In addition, the $t\bar{t}\gamma$ signature is an important control sample for $t\bar{t}Z$ and $t\bar{t}H$, $H \rightarrow \gamma\gamma$ analyses.

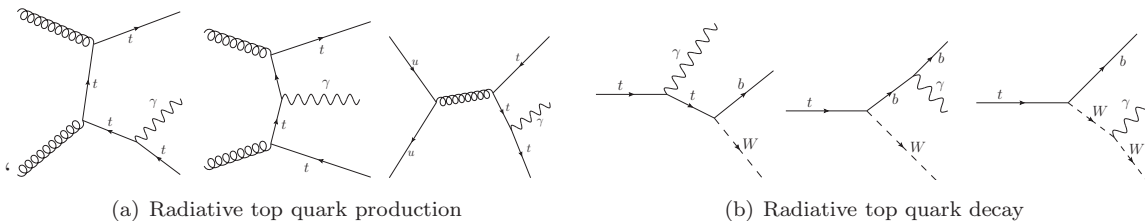


Figure 5. Representative Feynman diagrams for the $t\bar{t}\gamma$ process. Radiative top quark decay diagrams also include radiation from decay products of the W .

The distinction between the two classes of processes is indispensable for determination of couplings of the top quark to the photon as discussed below. However, the analyses performed so far by CDF and ATLAS collaborations didn't measure the couplings, providing instead measurements of the $t\bar{t}\gamma$ cross section, $\sigma_{t\bar{t}\gamma}$. In both the CDF and ATLAS $t\bar{t}\gamma$ analyses the strategy is to perform data-driven background estimates for jets misidentified as electrons, and for jets and electrons misidentified as photons. In addition, the $t\bar{t}$ and $W\gamma$ production processes are used as control samples for the $t\bar{t}$ part of the event and for the photons, respectively. $Z \rightarrow e^+e^-$ with one of the electrons misidentified as a photon is used to estimate the $e \rightarrow \gamma$ fake rate both in ATLAS and CDF. Both ATLAS and CDF use the $Z \rightarrow e^+e^-$ process for real photons template, assuming similarity between electrons and photons in the electromagnetic calorimeter. CDF also uses $Z\gamma$ together with $W\gamma$ for further photon identification optimization.

The CDF collaboration published the first experimental evidence for $t\bar{t}\gamma$ production by measuring the $\sigma_{t\bar{t}\gamma}$ and the ratio $R = \sigma_{t\bar{t}\gamma}/\sigma_{t\bar{t}}$ with data corresponding to 6.0 fb^{-1} of $p\bar{p}$ collisions at $\sqrt{s} = 1.96$ TeV at the Tevatron. The $t\bar{t}\gamma$ cross section was measured to be $\sigma_{t\bar{t}\gamma} = 0.18 \pm 0.08 \text{ pb}$ with a significance of 3.0σ [72] for a photon $p_T > 6 \text{ GeV}$ (using a photon $p_T > 10 \text{ GeV}$ in the reconstruction). The ratio was measured to be $R = 0.024 \pm 0.009$ in a good agreement with the SM expectation of 0.024 ± 0.005 for a charge $2/3$ top quark. The dominant uncertainty in these measurements arises from the finite statistics of $t\bar{t}\gamma$ candidate events. However, the $R = \sigma_{t\bar{t}\gamma}/\sigma_{t\bar{t}}$ measurement is more precise than the $\sigma_{t\bar{t}\gamma}$ measurement due to the cancellation of the $t\bar{t}$ -related systematic uncertainties.

The ATLAS collaboration has performed the first $t\bar{t}\gamma$ production [73] cross section measurement at the LHC in 1.04 fb^{-1} of data at $\sqrt{s} = 7 \text{ TeV}$, $\sigma_{t\bar{t}\gamma} = 2.0 \pm 0.5 \text{ (stat.)} \pm 0.7 \text{ (syst.)} \pm 0.08 \text{ (lumi.) pb}$ for a photon p_T threshold of 8 GeV (using a photon $p_T > 15 \text{ GeV}$ in the reconstruction). The significance of the measurement is 2.7σ , and the measured cross section is in good agreement with the SM expectation of $2.1 \pm 0.4 \text{ pb}$ for a charge $2/3$ top quark. The uncertainty of the measurement is dominated by the photon identification efficiency, the initial and final state radiation modeling and the jet energy scale systematics. The analysis is being updated with the full 7 TeV dataset (systematic uncertainties are also expected to get reduced).

The LO $t\bar{t}\gamma$ production cross section increases by a factor of 5 from 7 TeV to 14 TeV center-of-mass

energy for photons with $p_T > 20$ GeV [74, 75]. With the much larger statistics expected after the upcoming 2013-2014 shutdown, analysis of the top quark–photon couplings is possible.

Furthermore, to isolate events with photon emission from top quarks, the photon radiation from the W and its decay products, as well as from the b quarks and from the initial-state quarks should be suppressed, as detailed in Ref. [76]. To suppress photon radiation from the b quarks (leptons) a large $\Delta R(\gamma, b)$ ($\Delta R(\gamma, \ell)$) is required. Photon emission from W decay products can be eliminated by requiring that the invariant mass of the $jj\gamma$ system $m(jj\gamma) > 90$ GeV and the $\ell\gamma\cancel{E}_T$ cluster transverse mass $m_T(\ell\gamma, \cancel{E}_T) > 90$ GeV. The radiation from the initial state quarks is hard to suppress without simultaneously reducing the signal cross section. However, as at the LHC $t\bar{t}$ production by gluon fusion dominates, it is not an issue (unlike at the Tevatron). In addition, the event is required to be consistent either with $t\bar{t}\gamma$ production, or with the $t\bar{t}$ production with radiative top decay by performing top quark and top quark + photon mass reconstruction as shown in Ref. [76].

Isolating events with photon emission from top quarks, as well as performing a ratio $R = \sigma_{t\bar{t}\gamma}/\sigma_{t\bar{t}}$ measurement to reduce $t\bar{t}$ -related systematic uncertainties is the strategy for future $t\bar{t}\gamma$ analyses. At the LHC, with 300 fb^{-1} several thousand signal events are expected, therefore precise determination of the $t\bar{t}\gamma$ couplings is possible [76] using the lepton plus jets channel. In addition, a precise $t\bar{t}\gamma$ couplings measurement can be performed using the dilepton channel which should provide a smaller systematic uncertainty (due to fewer jets in the event) but a slightly larger statistical uncertainty compared to the lepton plus jets channel. With 3000 fb^{-1} , differential measurements of $t\bar{t}\gamma$ couplings (for instance, as a function of photon p_T) as well as differential $t\bar{t}\gamma$ cross section measurements, can be performed.

4.3 $t\bar{t}Z$

The associated $t\bar{t}Z$ production is directly sensitive to $t\bar{t}Z$ couplings. Representative Feynman diagrams for $t\bar{t}V$ (in this Section $V = Z, W$) production are shown in Fig. 6.

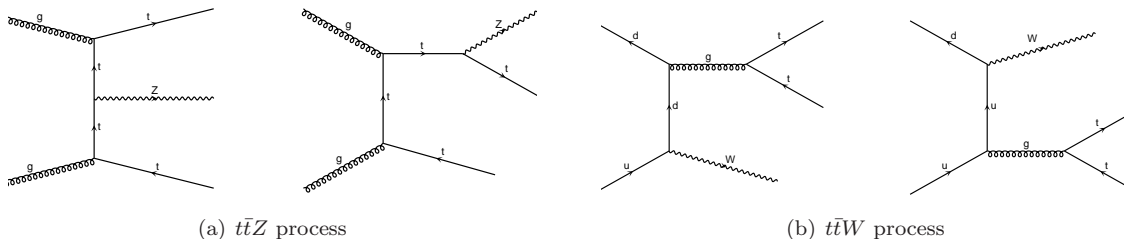


Figure 6. Representative Feynman diagrams for the $t\bar{t}V$ process.

The associated production of $t\bar{t}$ and Z or W bosons has been measured by CMS in 5 fb^{-1} of pp collisions at $\sqrt{s} = 7$ TeV [77]. The measurements exploit the fact that SM events with two prompt same-sign isolated leptons in the final state, as well as trilepton events, are very rare. A data-driven estimation procedure is employed to estimate the background contribution of jets misidentified as leptons.

A direct measurement of the $t\bar{t}Z$ cross section $\sigma_{t\bar{t}Z} = 0.28^{+0.14}_{-0.11}(\text{stat.})^{+0.06}_{-0.03}(\text{syst.})$ pb is obtained in the *trilepton channel*, observing 9 events with the expected background of 3.2 ± 0.8 events. The signal significance is 3.3 standard deviations from the background hypothesis. In the *dilepton channel* a total of 16 events is selected in the data, compared to an expected background contribution of 9.2 ± 2.6 events. The presence of a $t\bar{t}V$ ($V = W, Z$) signal is established with a significance of 3.0 standard

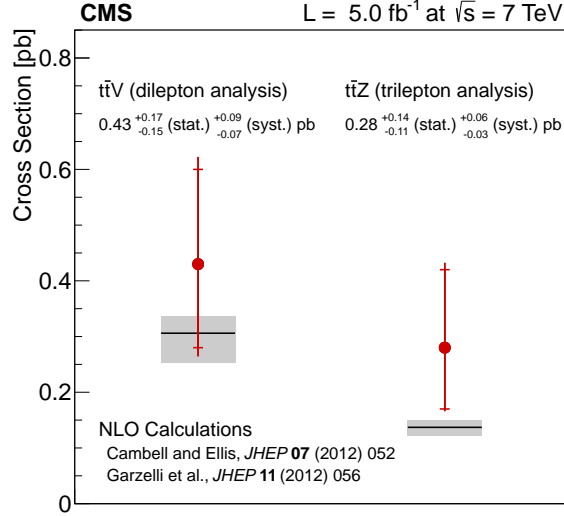


Figure 7. Measurements of the $t\bar{t}Z$ and $t\bar{t}V$ production cross sections [77], in the same-sign dilepton (left) and trilepton channel (right), respectively. The measurements are compared to the next-to-leading order Standard Model calculation (horizontal black lines) and their uncertainty (grey bands). Internal error bars for the measurements represent the statistical component of the uncertainty.

deviations. The $t\bar{t}V$ process cross section is measured to be $\sigma_{t\bar{t}V} = 0.43_{-0.15}^{+0.17}(\text{stat.})_{-0.07}^{+0.09}(\text{syst.})$ pb. Both $\sigma_{t\bar{t}V}$ and $\sigma_{t\bar{t}Z}$ cross section measurements are compatible with the NLO predictions. These results are shown in Fig. 7 together with the next-to-leading order SM predictions.

The ATLAS collaboration also performed $t\bar{t}Z$ analysis [8], using a much tighter selection to suppress backgrounds, that resulted in observing one event in data and setting a limit $\sigma_{t\bar{t}Z} < 0.71$ pb at 95% CL consistent with the CMS measurement and with theoretical predictions [78].

The uncertainties of the $t\bar{t}Z$ measurements up to date are dominated by statistics. The LO $t\bar{t}Z$ production cross section increases by a factor of ~ 1.4 from 7 TeV to 8 TeV center-of-mass energy [74, 75], so the expected decrease in the statistical uncertainty with the dataset collected in 2012 is a factor of 2.5. Therefore, statistical uncertainties are expected to dominate the $\sigma_{t\bar{t}V}$ and $\sigma_{t\bar{t}Z}$ measurements performed with 2012 data.

However, the LO $t\bar{t}Z$ production cross section increases by roughly an order of magnitude from 7 TeV to 14 TeV center-of-mass energy [74, 75], therefore precise measurements of the $t\bar{t}Z$ production cross section can be performed after the 2013-2014 shutdown. According to Ref. [76], with 300 fb^{-1} of 14 TeV collisions data, the $t\bar{t}Z$ vector (axial vector) coupling can be determined with an uncertainty of 45 – 85% (15 – 20%), whereas the dimension-five dipole form factors can be measured with a precision of 50 – 55%. For 3000 fb^{-1} of data expected at the High Luminosity (HL) LHC, the limits are expected to improve by a factor of 3.

4.4 Linear Collider prospects⁵

A future e^+e^- collider [79, 80] operated at center-of-mass energy greater than the top quark pair production threshold ($\sqrt{s} > 2m_t$) offers excellent prospects for a precision top physics programme.

⁵Author: Marcel Vos, IFIC (UVEG/CSIC)

One of the key assets of lepton collider is calculability; many observable quantities can be predicted at the per mil level. The $t\bar{t}$ production rate can be calculated to excellent precision. For $\sqrt{s} = 500$ GeV QCD corrections have been determined to order α_s^3 [81]. The N^4LO contribution to the rate is estimated from scale variations to be approximately 3 per mil.

Top quark production at an e^+e^- collider is less copious than at the LHC. At the LC $e^+e^- \rightarrow Z/\gamma^* \rightarrow t\bar{t}$ is the dominant top quark production process. All $t\bar{t}$ final states are readily isolated, with background levels due to other six-fermion processes below 5%. At $\sqrt{s} = 500$ GeV the (unpolarized) cross-section is approximately 0.6 pb. At that energy an integrated luminosity of 125pb^{-1} is envisaged to be accumulated each year. A four year period thus yields a sample of several 100,000 top quark pairs, shared equally between two beam polarization configurations ($\mathcal{P}_1^-, \mathcal{P}_1^+ = \pm 80\%, \mp 30\%$).

The LC potential for the characterization of the $t\bar{t}Z$ and $t\bar{t}\gamma$ vertices was established using parton-level studies a long time ago [82]. For compatibility with these studies and the LHC prospects of Reference [76] we express the sensitivity in terms of the form factors that characterize the current at the $t\bar{t}Z$ and $t\bar{t}\gamma$ vertices:

$$\Gamma_\mu^{t\bar{t}X}(k^2, q, \bar{q}) = ie \left\{ \gamma_\mu \left(\tilde{F}_{1V}^X(k^2) + \gamma_5 \tilde{F}_{1A}^X(k^2) \right) + \frac{(q - \bar{q})_\mu}{2m_t} \left(\tilde{F}_{2V}^X(k^2) + \gamma_5 \tilde{F}_{2A}^X(k^2) \right) \right\} \quad (4.1)$$

Recently, the LC prospect were revisited [83, 84] with a detailed simulation of the detector response, including the impact of $\gamma\gamma \rightarrow \text{hadrons}$ background. The analysis aims for simultaneous determination of the photon and Z boson form factors. Three observables - the cross section, the forward-backward asymmetry and the top quark polarization - are evaluated for two polarization states of the electron and positron beams. These six independent measurements are used to extract five CP conserving form factors: $\tilde{F}_{1V}^{\gamma,Z}$ and $\tilde{F}_{2V}^{\gamma,Z}$ and \tilde{F}_{1A}^Z (F_{1A}^γ is taken to be 0 to preserve gauge invariance).

After accounting for the selection efficiency the statistics of the sample is sufficient to reduce the statistical uncertainty of these measurements to the per mil level. Systematic errors due to the reconstruction of the complex $t\bar{t}$ events are accounted for. The impact of a number of several other potential sources - such as the expected error on the beam energy, the luminosity and the beam polarization - is evaluated and found to be sub-dominant.

The results are compared to the LHC prospects from Reference [85] (assuming an integrated luminosity of 300fb^{-1} at 14 TeV) in Figure 8 and Table 3. The estimated sensitivity of the LC is an order of magnitude greater for all couplings than that expected at the LHC, and exceeds it by two orders of magnitude for the vectorial couplings of the Z boson.

The control over the beam polarization proves sufficient to disentangle photon and Z boson form factors. A simultaneous extraction of \tilde{F}_1 and \tilde{F}_2 , independent of any assumption on the other form factor, turns out to be more cumbersome. Therefore, the results in Figure 8 correspond to a simultaneous determination of the four \tilde{F}_1 form factors, while the two \tilde{F}_2 form factors are kept at their Standard Model values, and vice versa. The potential to disentangle \tilde{F}_1 and \tilde{F}_2 improves at larger center-of-mass energy. The study of Reference [42] shows that the equivalent effective operators can be constrained simultaneously if measurements at $\sqrt{s} = 500$ GeV are combined with measurements at 1 TeV.

The potential of the LC to uncover Beyond the Standard Model contributions to the top quark electric and magnetic dipole moment has not yet been evaluated in full simulation. The estimates at parton-level from Reference [82] are compared to the LHC prospects in Table 3.

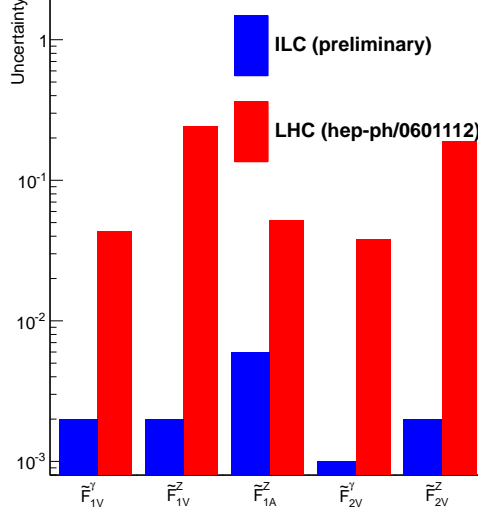


Figure 8. Sensitivity at 68.3% CL for CP conserving form factors $\tilde{F}_{1V,A}^X$ and \tilde{F}_{2V}^X defined in Eq. 4.1 at the LHC and at linear e^+e^- colliders.

Coupling	SM value	LHC [85]	e^+e^- [82]	e^+e^- [83, 84]
		$\mathcal{L} = 300 \text{ fb}^{-1}$	$\mathcal{L} = 300 \text{ fb}^{-1}$	$\mathcal{L} = 500 \text{ fb}^{-1}$
			$\mathcal{P}, \mathcal{P}' = -0.8, 0$	$\mathcal{P}, \mathcal{P}' = \pm 0.8, \mp 0.3$
$\Delta \tilde{F}_{1V}^\gamma$	0.66	+0.043 -0.041	-	+0.002 -0.002
$\Delta \tilde{F}_{1V}^Z$	0.23	+0.240 -0.620	+0.004 -0.004	+0.002 -0.002
$\Delta \tilde{F}_{1A}^Z$	-0.59	+0.052 -0.060	+0.009 -0.013	+0.006 -0.006
$\Delta \tilde{F}_{2V}^\gamma$	0.015	+0.038 -0.035	+0.004 -0.004	+0.001 -0.001
$\Delta \tilde{F}_{2V}^Z$	0.018	+0.270 -0.190	+0.004 -0.004	+0.002 -0.002
$\Delta \text{Re } \tilde{F}_{2A}^\gamma$	-	+0.17 -0.17	+0.007 -0.007	
$\Delta \text{Re } \tilde{F}_{2A}^Z$	-	+0.35 -0.35	+0.008 -0.008	
$\Delta \text{Im } \tilde{F}_{2A}^\gamma$	-	+0.17 -0.17	+0.008 -0.008	
$\Delta \text{Im } \tilde{F}_{2A}^Z$	-	+0.035 -0.035	+0.015 -0.015	

Table 3. Sensitivity at 68.3% CL for CP conserving form factors $\tilde{F}_{1V,A}^X$ and \tilde{F}_{2V}^X and the top quark magnetic and electric dipole form factors \tilde{F}_{2A}^V of Eq. 4.1. LHC prospects are compared to two linear e^+e^- collider studies. The assumptions for the integrated luminosity and, for e^+e^- colliders, the beam polarisation, are indicated in the table header.

Summarizing: an e^+e^- collider with $\sqrt{s} > 2m_t$ offers a powerful precision top physics programme. The sensitivity for anomalous electroweak couplings of the top quark is boosted by an order of magnitude with respect to the expected LHC potential.

5 Coupling of the Top quark to the Higgs boson⁶

With the decades-long search for the Higgs boson complete and a resonance consistent with Standard Model (SM) Higgs boson production observed [86–88], the era of precision Higgs boson studies now begins. One particularly important property of the Higgs boson is its coupling to top quarks. By far the most massive quark, as well as the most massive fundamental particle observed to-date, the top quark has Yukawa couplings close to unity, making (first observation and then) measurements of $t\bar{t}H$ particularly important. $H \rightarrow \gamma\gamma$ measurements from both ATLAS and CMS [89, 90], which show larger signal strength than expected in the SM in a channel with non-zero contributions from loops involving top quarks, make a measurement of the top-Higgs coupling even more important.

Measurements of the $t\bar{t}H$ final state are not trivial, as the $t\bar{t}$ system itself is already quite complicated. Due to small cross sections for $t\bar{t}H$ production when compared with non-associated Higgs production (or even when compared with ZH and WH production), analyses so far have only searched for $t\bar{t}H$ production with subsequent $H \rightarrow b\bar{b}$ decay, which gives the largest branching fraction. The final state is thus $t\bar{t} + b\bar{b}$ with a resonance in the $b\bar{b}$ mass. The main irreducible background is then $t\bar{t}$ production in association with extra jets, typically of heavy flavor.

5.1 Searches for $t\bar{t} + H$

There are four direct searches in the literature for $t\bar{t}H$ production. CMS sets the most stringent limits, with an observed (expected) upper limit at 95% confidence level (C.L.) of 4.6x (3.8x) the SM expectation [91] using the full 2011 LHC $\sqrt{s} = 7$ TeV data set (5 fb^{-1}). The analysis uses both the lepton+jets and dilepton topologies of $t\bar{t}$ decay. ATLAS also uses the full 2011 data set (4.7 fb^{-1}) and sets observed (expected) upper limits of 13.1x (10.5x) the SM expectation [92] at 95 % C.L., using only the single lepton decay channel. CDF has two analyses: the full Run II Tevatron data set (9.45 fb^{-1}) is used in the single lepton topology, with corresponding observed (expected) upper limits of 20.5x (12.6x) the SM expectation [93] at 95 % C.L. A second CDF analysis [94] examines 0-lepton events to capture both all-hadronic $t\bar{t}$ decays and single lepton decays where the lepton was not reconstructed. The analysis is unique, but suffers from extremely large backgrounds (from QCD), and in 5.7 fb^{-1} sets observed (expected) upper limits of 36.2x (26.2x) the SM prediction at a Higgs boson mass of 125 GeV.

The CMS analysis begins with the separation of events into single lepton and dilepton categories. Tight leptons are required to be above 30 GeV. The definition of Loose leptons has relaxed identification, isolation and $|\eta|$ requirements, and also lowers the p_T thresholds to 10 (15-20) GeV for muons (electrons). Single lepton events are required to contain tight leptons, whereas dilepton events can contain one loose and one tight lepton. The 3 leading jets are required to be above 40 GeV, and any additional jets are required to have $p_T > 30$ GeV. Events are further separated based on the number of jets and tags: 4 jets (3 or ≥ 4 tags), 5 jets (3 or ≥ 4 tags) and 6 or more jets (2, 3 or ≥ 4 tags) in the single lepton category; and 2 jets (2 tags) and ≥ 3 jets (≥ 3 tags) in the dilepton category. Artificial neural networks (ANN) are trained separately in each category to separate signal and background. Inputs to the ANNs include shape information (sphericity and aplanarity), b -tag weights (to separate out $t\bar{t}$ +light flavor from $t\bar{t}$ +production of extra associated heavy flavor), several Fox-Wolfram moments, event mass, jet p_T , ΔR between tagged jets, ΔR between leptons and jets, and the number of jets. Major systematic uncertainties considered include jet energy scale (JES), scale uncertainties for $t\bar{t}$ production (evaluated by changing factorization and renormalization scales up and

⁶Author: Jahred Adelman, Yale University

down by factors of two in Madgraph, leading to uncertainties of 0-20%) and b -tag scale factor (SF) uncertainties. When scales are changed, the variations are treated as uncorrelated between $t\bar{t}$ +light flavor jets, $t\bar{t}b\bar{b}$ and $t\bar{t}c\bar{c}$, and give uncertainties that vary as a function of the number of jets. For the lepton+jets channel, the b -tag SF uncertainty is the dominant systematic effect. For the dilepton channel, the factorization scale is the dominant systematic uncertainty.

The ATLAS analysis examines only single lepton events. Electrons (muons) are required to be above 25 (20) GeV. Jets are required to have p_T above 25 GeV. In the electron channel, $\cancel{E}_T > 30$ GeV and the transverse mass (m_T) between the lepton and the \cancel{E}_T is also required to be above 30 GeV. In the muon channel, $\cancel{E}_T > 20$ GeV and $\cancel{E}_T + m_T > 60$ GeV. Events are categorized based on the number of jets and number of b -tags. The five control regions are: 4 jets (0, 1 or ≥ 2 tags), 5 jets (2 tags) and 6 or more jets (2 tags). The four signal categories are: 5 jets (3 or ≥ 4 tags) and ≥ 6 jets (3 or ≥ 4 tags). The final observable in the ≥ 6 -jet signal regions are the invariant mass of the pair of jets ($m_{b\bar{b}}$) not selected to come from $t\bar{t}$ decay. A kinematic fit for the $t\bar{t}$ hypothesis is used to assign observed jets to partons. Transfer functions are used to describe detector resolution for jets matched to partons at the truth level. The scalar sum of the jet p_T is used as an observable in the 5-jet signal region and in the control regions both to gain statistical power and also to help constrain nuisance parameters *in-situ* in the fit to data. Major systematic uncertainties considered include jet energy scale (JES), b -tag SF uncertainties, and scale uncertainties for $t\bar{t}$ production. Scale uncertainties have two factorization scale uncertainties (evaluated by varying the default factorization scale $Q^2 = \Sigma_{\text{partons}}(m^2 + p^2)$ up and down by factors of two and taking the larger difference from nominal, as well as by using an alternative default scale $Q^2 = x_1x_2s$, which dominates). The renormalization scale uncertainty is evaluated by varying the scale up and down by factors of factors of two. When varying scale uncertainties, the fraction of $t\bar{t}$ +jets events with heavy flavor is found to vary by $\pm 50\%$, which is taken as an additional uncertainty.

The single lepton CDF measurement requires a single electron or muon above 18 GeV and $\cancel{E}_T > 10 - 25$ GeV, depending on the lepton flavor and $|\eta|$. Jets are required to have $p_T > 20$ GeV. Events are categorized based on the number of jets (4,5,6), with each jet category further split into 5 different b -tag subcategories using two different tagging algorithms. ANNs are trained in each subcategory to separate signal and background. The 18 input variables include \cancel{E}_T , jet p_T values, event mass, ΔR between tagged jets, lepton-jet masses, and dijet masses. The 4-jet 2-tag category is used to validate the ANN. Dominant systematic uncertainties are b -tag SFs, JES uncertainties, and background normalizations. A 10% uncertainty is assumed on the $t\bar{t}$ + jets normalization, and a 100% uncertainty is assumed on the $t\bar{t}b\bar{b}$ normalization.

As mentioned above, large uncertainties appear in these searches from normalization of $t\bar{t}$ produced in association with extra heavy flavor jets, the dominant background in the signal-enriched regions. CMS has made the first measurement of the ratio of production cross sections: $\sigma(t\bar{t}b\bar{b})/\sigma(t\bar{t}jj)$ in a given visible phase space [95]. The result is larger than predictions from MADGRAPH and POWHEG, though with large uncertainties. Longer term and with significantly higher luminosities, the top-Higgs coupling will be better measured in other channels. Two promising examples are the diphoton and dimuon decay channels, where the presence of the Higgs boson produced in association with $t\bar{t}$ is seen via a resonance. ATLAS studied these channels [96] with hypothetical 300 and 3000 fb^{-1} data sets containing large pile up at $\sqrt{s} = 14\text{TeV}$, and claims the ability to measure $\Delta(\Gamma_t/\Gamma_g)$ to better than 55% (25%) with 300 (3000) fb^{-1} .

6 Top quark + jets⁷

A measurement of $t\bar{t}$ production with additional jets is an important test of perturbative QCD at the LHC energy scale. The production of $t\bar{t}$ +jets is sensitive to initial and final state radiation as well as to other details of the $t\bar{t}$ production modelling. As such, it can serve as verification of theoretical models and help to tune Monte Carlo generators. Studies of $t\bar{t}$ +jets may reduce systematic uncertainty due to additional quark/gluon production, which is important for many searches for new physics.

The first $t\bar{t}$ +jets measurement was performed at the Tevatron by the CDF collaboration [97]. At the LHC, both ATLAS and CMS experiments studied the $t\bar{t}$ +jets production in detail. The studies performed at the LHC include measurement of $t\bar{t}$ production with a veto on additional central jet activity [98, 99]; study of jet multiplicity in $t\bar{t}$ events [99–101]; the $t\bar{t}$ +jets cross section measurement [102]; and measurement of heavy flavor composition of $t\bar{t}$ events [103].

At hadron colliders, top quarks are predominantly produced in pairs. In the Standard Model, a top quark decays almost 100% of the time to a W boson and a b quark. The W boson can further decay leptonically (to a lepton and a neutrino) or hadronically (giving rise to a pair of jets). Consequently, there are three possible $t\bar{t}$ final states: both W 's decay leptonically (dilepton channel), one W decays leptonically and the other one hadronically (lepton+jets channel), or both W 's decay hadronically (all-hadronic channel). All analyses described below are looking at top quark pairs produced in either dilepton or lepton+jets channel.

6.1 $t\bar{t}$ with central jet veto

ATLAS measured [98] the fraction of $t\bar{t}$ events produced without additional jet(s) in a certain rapidity interval⁸. The measured quantity f (gap fraction) is defined as $f(x) = n(x)/N$, where N is the total number of selected $t\bar{t}$ events, and $n(x)$ is the number of selected $t\bar{t}$ events with additional jet veto. The results were obtained for two veto definitions: $x = Q_0$ (no additional jets with transverse momentum p_T above threshold Q_0 in a certain rapidity interval), and $x = Q_{\text{sum}}$ (the scalar transverse momentum sum of the additional jets in the rapidity interval is less than Q_{sum}). By measuring the ratio of production rates, many systematic uncertainties cancel out, which makes the result more sensitive to Monte Carlo modelling parameters.

The gap fraction distributions as functions of x (with a minimum x value of 25 GeV) were obtained for four jet rapidity intervals: $|y| < 0.8$, $0.8 \leq |y| < 1.5$, $1.5 \leq |y| < 2.1$, and for the full rapidity range, $|y| < 2.1$. The measurement was performed in the dilepton channel at a center-of-mass energy of 7 TeV, using 2.05 fb^{-1} of integrated luminosity. The obtained gap fraction was corrected to the particle level using a correction factor defined as the ratio of the particle level gap fraction to the reconstructed gap fraction.

The results were compared to theoretical models implemented in MC@NLO [104, 105] interfaced to HERWIG [106] and JIMMY [107], POWHEG [108, 109] interfaced to either PYTHIA [110] or HERWIG/JIMMY, ALPGEN [111] interfaced to HERWIG/JIMMY, and SHERPA [112]. It was found that while all models describe the data reasonably well within the full $|y| < 2.1$ veto interval, they tend to predict too much jet activity in the most forward $1.5 \leq |y| < 2.1$ region. In addition, MC@NLO underestimates the data in the central region $|y| < 0.8$.

A similar measurement (rapidity gap as a function of Q_0 and Q_{sum} unfolded to the particle level) was done by CMS [99] in the dilepton channel with 5 fb^{-1} of 7 TeV data. The rapidity gap

⁷Author: Sasha Khanov, OK State University

⁸Rapidity is defined as $y = 0.5 \ln[(E + p_z)(E - p_z)]$ where E is the energy and p_z is the component of the momentum along the beam direction.

distributions were determined for the whole jet rapidity range ($|y| < 2.4$) and compared to predictions from MADGRAPH [113] and POWHEG interfaced to PYTHIA, and MC@NLO interfaced to HERWIG. The best description was obtained with MC@NLO, while it was observed that increasing the Q^2 scale in MADGRAPH improves the agreement between the data and the simulation.

6.2 Jet multiplicity in $t\bar{t}$ events and $t\bar{t}$ +jet production cross section

The first measurement of the cross section of $t\bar{t}$ with an additional jet was performed at CDF using 4.1 fb^{-1} of integrated luminosity [97]. The measurement was performed in the lepton+jets channel, with a 2D likelihood discriminant formed to simultaneously measure the $t\bar{t}$ +jet and $t\bar{t}$ +(no jet) cross sections. The result $\sigma(t\bar{t} + j) = 1.6 \pm 0.2(\text{stat.}) \pm 0.5(\text{syst.}) \text{ pb}$ was found to be in a good agreement with next-to-leading order QCD calculations.

The jet multiplicity distribution in $t\bar{t}$ events was measured by ATLAS in the lepton+jet channel and by CMS in the lepton+jet and dilepton channels. Both sets of results were obtained at a center-of-mass energy of 7 TeV, using 4.7 fb^{-1} (ATLAS) and 5 fb^{-1} (CMS) of integrated luminosity. ATLAS measured [100] the jet multiplicity for four values of the jet transverse momentum threshold (25, 40, 60, and 80 GeV). The results were unfolded to the particle level with a response matrix $M_{\text{part}}^{\text{reco}}$ applied iteratively using Bayesian unfolding [114]. The resulting jet multiplicity distributions were found to be consistent with ALPGEN interfaced with PYTHIA and HERWIG, as well as POWHEG interfaced with PYTHIA. As expected, the data disfavors the MC@NLO model, which predicts lower jet multiplicity and softer jets.

CMS measured [99] jet multiplicity in the dilepton channel for two jet transverse momentum thresholds (30 and 60 GeV). The results were corrected to the particle level using a regularised unfolding method [115, 116]. The resulting distributions were compared to Monte Carlo predictions. As in the ATLAS analysis, it was found that MC@NLO interfaced to HERWIG generates lower multiplicities than observed. MADGRAPH and POWHEG interfaced to PYTHIA describe the data with up to six additional jets well.

In the lepton+jet analysis [101], CMS measured normalized differential cross section defined as the measured cross section in each jet multiplicity bin divided by the measured total cross section in the same phase space. The results were compared to predictions from various Monte Carlo generators with conclusions similar to those from the dilepton analysis.

ATLAS performed [102] a measurement of the cross section for production of $t\bar{t}$ with additional jets (denoted $t\bar{t}j$) in the lepton+jets channel with 4.7 fb^{-1} of 7 TeV data. Two definitions of $t\bar{t}j$ events were considered, both based on particle jets from the Monte Carlo model. In definition 1, events were declared $t\bar{t}j$ if at least one particle jet could not be matched to a parton from a top quark. In definition 2, all events with at least five particle jets were termed $t\bar{t}j$. The $t\bar{t}j$ production cross sections were obtained by matching the Monte Carlo predictions for $t\bar{t}j$ and non- $t\bar{t}j$ events against the data. The cross section for $t\bar{t}$ production in association with at least one additional jet according to definition 1 is measured to be $\sigma_{t\bar{t}j} = 102 \pm 2(\text{stat.})_{-25}^{+23}(\text{syst.}) \text{ pb}$, and its ratio to the $t\bar{t}$ inclusive cross section is $\sigma_{t\bar{t}j}/\sigma_{t\bar{t}}^{\text{incl}} = 0.54 \pm 0.01(\text{stat.})_{-0.08}^{+0.05}(\text{syst.})$.

6.3 $t\bar{t}$ +jets heavy flavor composition

A first measurement of the cross section ratio $\sigma(t\bar{t}b\bar{b})/\sigma(t\bar{t}jj)$ was done by CMS [103] in the dilepton channel using 5 fb^{-1} of integrated luminosity collected at a center-of-mass-energy of 7 TeV. The result was obtained by fitting the b -tagged jet multiplicity distributions and correcting to particle level. The resulting ratio was found to be $\sigma(t\bar{t}b\bar{b})/\sigma(t\bar{t}jj) = 3.6 \pm 1.1(\text{stat.}) \pm 0.9(\text{syst.})\%$ which can be compared

to predictions from MADGRAPH (1.2%) and POWHEG (1.3%). The result cannot be directly compared to NLO QCD calculations as the particle-to-parton correction would be required.

Summary

Overview on top couplings measurements is presented, and the prospects of future measurements are discussed. With the advent of high statistics top physics at the LHC with 300 fb^{-1} and at the high-luminosity LHC with 3000 fb^{-1} , the processes where the bosons (photon, Z and Higgs) are produced in association with top quarks become accessible. The first evidence on the coupling of the top quark to these particles will come from the production rate, followed by precision measurements.

Acknowledgments

The research of RKE is supported by the US DOE under contract DE-AC02-06CH11357. MB is supported by DOE grant DE-FG-03-91ER40682.

References

- [1] F.-P. Schilling, *Top Quark Physics at the LHC: A Review of the First Two Years*, *Int.J.Mod.Phys.* **A27** (2012) 1230016 [[1206.4484](#)].
- [2] T. M. Liss, *Top Quark Properties*, [1212.0489](#).
- [3] **CDF Collaboration**, T. Aaltonen *et. al.*, *Evidence for $t\bar{t}\gamma$ Production and Measurement of $\sigma_{t\bar{t}\gamma}/\sigma_{t\bar{t}}$* , *Phys.Rev.* **D84** (2011) 031104 [[1106.3970](#)].
- [4] **ATLAS Collaboration**, *Measurement of the inclusive $t\bar{t}\gamma$ cross section with the ATLAS detector*, [ATLAS-CONF-2011-153](#).
- [5] K. Melnikov, M. Schulze and A. Scharf, *QCD corrections to top quark pair production in association with a photon at hadron colliders*, *Phys.Rev.* **D83** (2011) 074013 [[1102.1967](#)].
- [6] D. Peng-Fei, Z. Ren-You, M. Wen-Gan, H. Liang, G. Lei *et. al.*, *Next-to-leading order QCD corrections to $t\bar{t}\gamma$ production at the 7 TeV LHC*, *Chin.Phys.Lett.* **28** (2011) 111401 [[1110.2315](#)].
- [7] **CMS Collaboration**, *Measurement of the Associated Production of Vector Bosons with Top-Antitop Pairs at 7 TeV*, [CMS-PAS-TOP-12-014](#).
- [8] **ATLAS Collaboration**, *Search for $t\bar{t}Z$ production in the three lepton final state with 4.7 fb^{-1} of $\sqrt{s} = 7\text{ TeV}$ pp collision data collected by the ATLAS detector*, [ATLAS-CONF-2012-126](#).
- [9] **ATLAS Collaboration**, G. Aad *et. al.*, *A search for flavour changing neutral currents in top-quark decays in pp collision data collected with the ATLAS detector at $\sqrt{s} = 7\text{ TeV}$* , *JHEP* **1209** (2012) 139 [[1206.0257](#)].
- [10] **CMS Collaboration**, S. Chatrchyan *et. al.*, *Search for flavor changing neutral currents in top quark decays in pp collisions at 7 TeV*, [1208.0957](#).
- [11] W. Beenakker, S. Dittmaier, M. Kramer, B. Plumper, M. Spira *et. al.*, *Higgs radiation off top quarks at the Tevatron and the LHC*, *Phys.Rev.Lett.* **87** (2001) 201805 [[hep-ph/0107081](#)].
- [12] L. Reina, S. Dawson and D. Wackerth, *QCD corrections to associated t anti- t h production at the Tevatron*, *Phys.Rev.* **D65** (2002) 053017 [[hep-ph/0109066](#)].
- [13] S. Dawson, C. Jackson, L. Orr, L. Reina and D. Wackerth, *Associated Higgs production with top quarks at the large hadron collider: NLO QCD corrections*, *Phys.Rev.* **D68** (2003) 034022 [[hep-ph/0305087](#)].

- [14] M. Garzelli, A. Kardos, C. Papadopoulos and Z. Trocsanyi, *Standard Model Higgs boson production in association with a top anti-top pair at NLO with parton showering*, *Europhys.Lett.* **96** (2011) 11001 [[1108.0387](#)].
- [15] R. Frederix, S. Frixione, V. Hirschi, F. Maltoni, R. Pittau *et. al.*, *Scalar and pseudoscalar Higgs production in association with a top-antitop pair*, *Phys.Lett.* **B701** (2011) 427–433 [[1104.5613](#)].
- [16] F. Maltoni, K. Paul, T. Stelzer and S. Willenbrock, *Associated production of Higgs and single top at hadron colliders*, *Phys.Rev.* **D64** (2001) 094023 [[hep-ph/0106293](#)].
- [17] V. Barger, M. McCaskey and G. Shaughnessy, *Single top and Higgs associated production at the LHC*, *Phys.Rev.* **D81** (2010) 034020 [[0911.1556](#)].
- [18] M. Farina, C. Grojean, F. Maltoni, E. Salvioni and A. Thamm, *Lifting degeneracies in Higgs couplings using single top production in association with a Higgs boson*, [1211.3736](#).
- [19] S. Biswas, E. Gabrielli and B. Mele, *Single top and Higgs associated production as a probe of the $Ht\bar{t}$ coupling sign at the LHC*, [1211.0499](#).
- [20] P. Agrawal, S. Mitra and A. Shivaji, *Effect of Anomalous Couplings on the Associated Production of a Single Top Quark and a Higgs Boson at the LHC*, [1211.4362](#).
- [21] **CDF** Collaboration, T. Aaltonen *et. al.*, *Measurement of W -Boson Polarization in Top-quark Decay using the Full CDF Run II Data Set*, [1211.4523](#).
- [22] **D0** Collaboration, V. M. Abazov *et. al.*, *Measurement of the W boson helicity in top quark decays using 5.4 fb^{-1} of $p\bar{p}$ collision data*, *Phys.Rev.* **D83** (2011) 032009 [[1011.6549](#)].
- [23] **CMS** Collaboration, *W helicity in top pair events*, [CMS-PAS-TOP-11-020](#).
- [24] **ATLAS** Collaboration, G. Aad *et. al.*, *Measurement of the W boson polarization in top quark decays with the ATLAS detector*, *JHEP* **1206** (2012) 088 [[1205.2484](#)].
- [25] **CDF, D0** Collaboration, T. Aaltonen *et. al.*, *Combination of CDF and D0 measurements of the W boson helicity in top quark decays*, *Phys.Rev.* **D85** (2012) 071106 [[1202.5272](#)].
- [26] **D0** Collaboration, V. M. Abazov *et. al.*, *Search for anomalous Wtb couplings in single top quark production in $p\bar{p}$ collisions at $\sqrt{s} = 1.96 \text{ TeV}$* , *Phys.Lett.* **B708** (2012) 21–26 [[1110.4592](#)].
- [27] **D0** Collaboration, V. M. Abazov *et. al.*, *Combination of searches for anomalous top quark couplings with 5.4 fb^{-1} of $p\bar{p}$ collisions*, *Phys.Lett.* **B713** (2012) 165–171 [[1204.2332](#)].
- [28] **ATLAS** Collaboration, G. Aad *et. al.*, *Measurement of the t -channel single top-quark production cross section in pp collisions at $\sqrt{s} = 7 \text{ TeV}$ with the ATLAS detector*, *Physics Letters B* **717** (2012) 330–350 [[1205.3130](#)].
- [29] E. Boos, L. Dudko and T. Ohl, *Complete calculations of $Wb\bar{b}$ and $Wb\bar{b} + \text{jet}$ production at Tevatron and LHC: Probing anomalous Wtb couplings in single top production*, *Eur.Phys.J.* **C11** (1999) 473–484 [[hep-ph/9903215](#)].
- [30] U. Baur, A. Juste, L. Orr and D. Rainwater, *Probing electroweak top quark couplings at hadron colliders*, *Phys.Rev.* **D71** (2005) 054013 [[hep-ph/0412021](#)].
- [31] U. Baur, A. Juste, D. Rainwater and L. Orr, *Improved measurement of $t\bar{t}Z$ couplings at the CERN LHC*, *Phys.Rev.* **D73** (2006) 034016 [[hep-ph/0512262](#)].
- [32] U. Baur, A. Juste, L. Orr and D. Rainwater, *Probing electroweak top quark couplings at hadron and lepton colliders*, *Nucl.Phys.Proc.Suppl.* **160** (2006) 17–21 [[hep-ph/0606264](#)].
- [33] J. Aguilar-Saavedra, *A Minimal set of top anomalous couplings*, *Nucl.Phys.* **B812** (2009) 181–204 [[0811.3842](#)].

- [34] C. Zhang and S. Willenbrock, *Effective-Field-Theory Approach to Top-Quark Production and Decay*, *Phys.Rev.* **D83** (2011) 034006 [[1008.3869](#)].
- [35] R. Yonamine, K. Ikematsu, T. Tanabe, K. Fujii, Y. Kiyo *et. al.*, *Measuring the top Yukawa coupling at the ILC at $\sqrt{s} = 500$ GeV*, *Phys.Rev.* **D84** (2011) 014033 [[1104.5132](#)].
- [36] Y. Bai, P. J. Fox and R. Harnik, *The Tevatron at the Frontier of Dark Matter Direct Detection*, *JHEP* **1012** (2010) 048 [[1005.3797](#)].
- [37] U. Haisch, F. Kahlhoefer and J. Unwin, *The impact of heavy-quark loops on LHC dark matter searches*, [1208.4605](#).
- [38] N. Greiner, S. Willenbrock and C. Zhang, *Effective Field Theory for Nonstandard Top Quark Couplings*, *Phys.Lett.* **B704** (2011) 218–222 [[1104.3122](#)].
- [39] C. Zhang, N. Greiner and S. Willenbrock, *Constraints on Non-standard Top Quark Couplings*, *Phys.Rev.* **D86** (2012) 014024 [[1201.6670](#)].
- [40] J. Drobnak, S. Fajfer and J. F. Kamenik, *Probing anomalous tWb interactions with rare B decays*, *Nucl.Phys.* **B855** (2012) 82–99 [[1109.2357](#)].
- [41] F. Bach and T. Ohl, *Anomalous Top Couplings at Hadron Colliders Revisited*, [1209.4564](#).
- [42] J. Aguilar-Saavedra, M. Fiolhais and A. Onofre, *Top Effective Operators at the ILC*, *JHEP* **1207** (2012) 180 [[1206.1033](#)].
- [43] J. Aguilar-Saavedra and J. Bernabeu, *W polarisation beyond helicity fractions in top quark decays*, *Nucl.Phys.* **B840** (2010) 349–378 [[1005.5382](#)].
- [44] Z. Hioki and K. Ohkuma, *Optimal-observable Analysis of Possible Non-standard Top-quark Couplings in $pp \rightarrow t\bar{t}X \rightarrow l^+ X'$* , *Phys.Lett.* **B716** (2012) 310–315 [[1206.2413](#)].
- [45] J. F. Kamenik, M. Papucci and A. Weiler, *Constraining the dipole moments of the top quark*, *Phys.Rev.* **D85** (2012) 071501 [[1107.3143](#)].
- [46] M. Baumgart and B. Tweedie, *A New Twist on Top Quark Spin Correlations*, [1212.4888](#).
- [47] J. Drobnak, S. Fajfer and J. F. Kamenik, *QCD Corrections to Flavor Changing Neutral Coupling Mediated Rare Top Quark Decays*, *Phys.Rev.* **D82** (2010) 073016 [[1007.2551](#)].
- [48] F. del Aguila, *Quark mixing: Determination of top couplings*, *Acta Phys.Polon.* **B30** (1999) 3303–3316 [[hep-ph/9911399](#)].
- [49] B. Lillie, J. Shu and T. M. Tait, *Top Compositeness at the Tevatron and LHC*, *JHEP* **0804** (2008) 087 [[0712.3057](#)].
- [50] N. Kidonakis, *Single top production at the Tevatron: Threshold resummation and finite-order soft gluon corrections*, *Phys.Rev.* **D74** (2006) 114012 [[hep-ph/0609287](#)].
- [51] N. Kidonakis, *Next-to-next-to-leading-order collinear and soft gluon corrections for t -channel single top quark production*, *Phys.Rev.* **D83** (2011) 091503 [[1103.2792](#)].
- [52] N. Kidonakis, *Two-loop soft anomalous dimensions for single top quark associated production with a W - or H -*, *Phys.Rev.* **D82** (2010) 054018 [[1005.4451](#)].
- [53] N. Kidonakis, *NNLL resummation for s -channel single top quark production*, *Phys.Rev.* **D81** (2010) 054028 [[1001.5034](#)].
- [54] **ATLAS** Collaboration, *Measurement of t -Channel Single Top-Quark Production in pp Collisions at $\sqrt{s} = 8$ TeV with the ATLAS detector*, [ATLAS-CONF-2012-132](#).

- [55] **ATLAS** Collaboration, G. Aad *et. al.*, *Measurement of the t -channel single top-quark production cross section in pp collisions at $\sqrt{s} = 7$ TeV with the ATLAS detector*, *Physics Letters B* **717** (2012) 330–350 [[1205.3130](#)].
- [56] **ATLAS** Collaboration, *Measurement of the t -channel single top-quark and top-antiquark production cross-sections and their ratio in pp collisions at $\sqrt{s} = 7$ TeV*, [ATLAS-CONF-2012-056](#).
- [57] **CMS** Collaboration, *Measurement of the single-top t -channel cross section in pp collisions at centre-of-mass energy of 8 TeV*, [CMS-PAS-TOP-12-011](#).
- [58] **CMS** Collaboration, S. Chatrchyan *et. al.*, *Measurement of the single-top-quark t -channel cross section in pp collisions at $\sqrt{s} = 7$ TeV*, [1209.4533](#).
- [59] **CDF** Collaboration, T. Aaltonen *et. al.*, *First Observation of Electroweak Single Top Quark Production*, *Phys.Rev.Lett.* **103** (2009) 092002 [[0903.0885](#)].
- [60] **D0** Collaboration, V. Abazov *et. al.*, *Observation of Single Top Quark Production*, *Phys.Rev.Lett.* **103** (2009) 092001 [[0903.0850](#)].
- [61] **CDF, D0** Collaboration, T. E. W. Group, *Combination of CDF and D0 Measurements of the Single Top Production Cross Section*, [0908.2171](#).
- [62] **D0** Collaboration, V. M. Abazov *et. al.*, *Measurements of single top quark production cross sections and $|V_{tb}|$ in $p\bar{p}$ collisions at $\sqrt{s} = 1.96$ TeV*, *Phys.Rev.* **D84** (2011) 112001 [[1108.3091](#)].
- [63] **CDF** Collaboration, CDF Collaboration, “Measurement of the t - t -bar + jet cross section with 4.1 fb^{-1} .” CDF Note 10793, 2010.
http://www-cdf.fnal.gov/physics/new/top/confNotes/cdf10793_SingleTop_7.5_public.pdf.
- [64] **CMS** Collaboration, S. Chatrchyan *et. al.*, *Evidence for associated production of a single top quark and W boson in pp collisions at 7 TeV*, *Phys.Rev.Lett.* (2012) [[1209.3489](#)].
- [65] **ATLAS** Collaboration, G. Aad *et. al.*, *Evidence for the associated production of a W boson and a top quark in ATLAS at $\sqrt{s} = 7$ TeV*, *Phys.Lett.* **B716** (2012) 142–159 [[1205.5764](#)].
- [66] T. M. Tait and C.-P. Yuan, *Single top quark production as a window to physics beyond the standard model*, *Phys.Rev.* **D63** (2000) 014018 [[hep-ph/0007298](#)].
- [67] **ATLAS** Collaboration, *Search for s -Channel Single Top-Quark Production in pp Collisions at $\sqrt{s} = 7$ TeV*, [ATLAS-CONF-2011-118](#).
- [68] **CMS** Collaboration, S. Chatrchyan *et. al.*, *Search for a W' boson decaying to a bottom quark and a top quark in pp collisions at $\sqrt{s} = 7$ TeV*, [1208.0956](#).
- [69] **ATLAS** Collaboration, G. Aad *et. al.*, *Search for tb resonances in proton-proton collisions at $\sqrt{s} = 7$ TeV with the ATLAS detector*, *Phys.Rev.Lett.* **109** (2012) 081801 [[1205.1016](#)].
- [70] **D0** Collaboration, V. M. Abazov *et. al.*, *Search for $W' \rightarrow tb$ resonances with left- and right-handed couplings to fermions*, *Phys.Lett.* **B699** (2011) 145–150 [[1101.0806](#)].
- [71] **CDF** Collaboration, T. Aaltonen *et. al.*, *Search for the Production of Narrow t anti- b Resonances in 1.9 fb^{-1} of p anti- p Collisions at $s^{*(1/2)} = 1.96$ -TeV*, *Phys.Rev.Lett.* **103** (2009) 041801 [[0902.3276](#)].
- [72] **CDF** Collaboration, T. Aaltonen *et. al.*, *Evidence for $t\bar{t}\gamma$ Production and Measurement of $\sigma_{t\bar{t}\gamma}/\sigma_{t\bar{t}}$* , *Phys.Rev.* **D84** (2011) 031104 [[1106.3970](#)].
- [73] **ATLAS** Collaboration, *Measurement of the inclusive t t -bar gamma cross section with the ATLAS detector*, [ATLAS-CONF-2011-153](#).
- [74] T. Stelzer and W. Long, *Automatic generation of tree level helicity amplitudes*, *Comput.Phys.Commun.* **81** (1994) 357–371 [[hep-ph/9401258](#)].

- [75] F. Maltoni and T. Stelzer, *MadEvent: Automatic event generation with MadGraph*, *JHEP* **0302** (2003) 027 [[hep-ph/0208156](#)].
- [76] U. Baur, A. Juste, L. Orr and D. Rainwater, *Probing electroweak top quark couplings at hadron colliders*, *Phys.Rev.* **D71** (2005) 054013 [[hep-ph/0412021](#)].
- [77] **CMS Collaboration** Collaboration, S. Chatrchyan *et. al.*, *Measurement of associated production of vector bosons and t t -bar at $\sqrt{s}= 7$ TeV*, [1303.3239](#).
- [78] U. Baur, A. Juste, D. Rainwater and L. Orr, *Improved measurement of ttZ couplings at the CERN LHC*, *Phys.Rev.* **D73** (2006) 034016 [[hep-ph/0512262](#)].
- [79] J. E. Brau, R. M. Godbole, F. R. L. Diberder, M. Thomson, H. Weerts *et. al.*, *The Physics Case for an $e+e-$ Linear Collider*, [1210.0202](#).
- [80] P. Lebrun, L. Linssen, A. Lucaci-Timoce, D. Schulte, F. Simon *et. al.*, *The CLIC Programme: Towards a Staged e^+e^- Linear Collider Exploring the Terascale : CLIC Conceptual Design Report*, [1209.2543](#).
- [81] Y. Kiyo, A. Maier, P. Maierhofer and P. Marquard, *Reconstruction of heavy quark current correlators at $O(\alpha(s)^{**3})$* , *Nucl.Phys.* **B823** (2009) 269–287 [[0907.2120](#)].
- [82] **ECFA/DESY LC Physics Working Group** Collaboration, J. Aguilar-Saavedra *et. al.*, *TESLA: The Superconducting electron positron linear collider with an integrated x-ray laser laboratory. Technical design report. Part 3. Physics at an $e+e-$ linear collider*, [hep-ph/0106315](#).
- [83] D. Asner, A. Hoang, Y. Kiyo, R. Pschl, Y. Sumino *et. al.*, *Top quark precision physics at the International Linear Collider*, [1307.8265](#).
- [84] M. Amjad, M. Boronat, T. Frisson, I. Garcia, R. Poschl *et. al.*, *A precise determination of top quark electro-weak couplings at the ILC operating at $\sqrt{s} = 500$ GeV*, [1307.8102](#).
- [85] A. Juste, Y. Kiyo, F. Petriello, T. Teubner, K. Agashe *et. al.*, *Report of the 2005 Snowmass top/QCD working group*, [hep-ph/0601112](#).
- [86] **ATLAS** Collaboration, G. Aad *et. al.*, *Observation of a new particle in the search for the Standard Model Higgs boson with the ATLAS detector at the LHC*, *Phys.Lett.* **B716** (2012) 1–29 [[1207.7214](#)].
- [87] **CMS** Collaboration, S. Chatrchyan *et. al.*, *Observation of a new boson at a mass of 125 GeV with the CMS experiment at the LHC*, *Phys.Lett.* **B716** (2012) 30–61 [[1207.7235](#)].
- [88] **TEVNPH (Tevatron New Phenomena and Higgs Working Group)**, **CDF** Collaboration, **D0** Collaboration, *Combined CDF and D0 Search for Standard Model Higgs Boson Production with up to 10.0 fb^{-1} of Data*, [1203.3774](#).
- [89] **ATLAS** Collaboration, *Observation of an excess of events in the search for the Standard Model Higgs boson in the gamma-gamma channel with the ATLAS detector*, [ATLAS-CONF-2012-091](#).
- [90] **CMS** Collaboration, *Evidence for a new state decaying into two photons in the search for the standard model Higgs boson in pp collisions*, [CMS-PAS-HIG-12-015](#).
- [91] **CMS** Collaboration, *Search for Higgs boson production in association with top quark pairs in pp collisions*, [CMS-PAS-HIG-12-025](#).
- [92] **ATLAS** Collaboration, *Search for the Standard Model Higgs boson produced in association with top quarks in proton-proton collisions at $s = 7$ TeV using the ATLAS detector*, [ATLAS-CONF-2012-135](#).
- [93] **CDF** Collaboration, T. Aaltonen *et. al.*, *Search for the standard model Higgs boson produced in association with top quarks using the full CDF data set*, *Phys.Rev.Lett.* **109** (2012) 181802 [[1208.2662](#)].
- [94] **CDF** Collaboration, *Search for SM Higgs boson production in association with $t\bar{t}$ using no lepton final state*, [CDF note 10582](#).

- [95] CMS Collaboration, *Search for SM Higgs boson production in association with $t\bar{t}$ using no lepton final state*, [CMS-PAS-TOP-12-024](#).
- [96] ATLAS Collaboration, *Physics at a High-Luminosity LHC with ATLAS (Update)*, [ATL-PHYS-PUB-2012-004](#).
- [97] CDF Collaboration, “Measurement of the $t\text{-}t\bar{t}$ + jet cross section with 4.1 fb^{-1} .” CDF Note 9850, 2009. http://www-cdf.fnal.gov/physics/new/top/2009/xsection/ttj_4.1invfb/.
- [98] ATLAS Collaboration, G. Aad *et. al.*, *Measurement of $t\bar{t}$ production with a veto on additional central jet activity in pp collisions at $\sqrt{s} = 7\text{ TeV}$ using the ATLAS detector*, *Eur.Phys.J.* **C72** (2012) 2043 [[1203.5015](#)].
- [99] *Measurement of Jet Multiplicity Distributions in Top Quark Events With Two Leptons in the Final State at a centre-of-mass energy of 7 TeV*, [CMS-PAS-TOP-12-023](#).
- [100] ATLAS Collaboration, *Measurement of the jet multiplicity in topanti-top final states produced in 7 TeV protonproton collisions with the ATLAS detector*, [ATLAS-CONF-2012-155](#).
- [101] CMS Collaboration, *Measurement of jet multiplicity in top pair events*, [CMS-PAS-TOP-12-018](#).
- [102] ATLAS Collaboration, *Measurement of the cross section for $t\bar{t}$ +jets production using a kinematic fit method with the ATLAS detector*, [ATLAS-CONF-2012-083](#).
- [103] CMS Collaboration, *First Measurement of the Cross Section Ratio $\sigma(t\bar{t}b\bar{b})/\sigma(t\bar{t}jj)$ in pp Collisions at $\sqrt{s} = 7\text{ TeV}$* , [CMS-PAS-TOP-12-024](#).
- [104] S. Frixione and B. R. Webber, *Matching NLO QCD computations and parton shower simulations*, *JHEP* **0206** (2002) 029 [[hep-ph/0204244](#)].
- [105] S. Frixione, P. Nason and B. R. Webber, *Matching NLO QCD and parton showers in heavy flavor production*, *JHEP* **0308** (2003) 007 [[hep-ph/0305252](#)].
- [106] G. Corcella, I. Knowles, G. Marchesini, S. Moretti, K. Odagiri *et. al.*, *HERWIG 6: An Event generator for hadron emission reactions with interfering gluons (including supersymmetric processes)*, *JHEP* **0101** (2001) 010 [[hep-ph/0011363](#)].
- [107] J. Butterworth, J. R. Forshaw and M. Seymour, *Multiparton interactions in photoproduction at HERA*, *Z.Phys.* **C72** (1996) 637–646 [[hep-ph/9601371](#)].
- [108] P. Nason, *A New method for combining NLO QCD with shower Monte Carlo algorithms*, *JHEP* **0411** (2004) 040 [[hep-ph/0409146](#)].
- [109] S. Frixione, P. Nason and C. Oleari, *Matching NLO QCD computations with Parton Shower simulations: the POWHEG method*, *JHEP* **0711** (2007) 070 [[0709.2092](#)].
- [110] T. Sjostrand, S. Mrenna and P. Z. Skands, *PYTHIA 6.4 Physics and Manual*, *JHEP* **0605** (2006) 026 [[hep-ph/0603175](#)].
- [111] M. L. Mangano, M. Moretti, F. Piccinini, R. Pittau and A. D. Polosa, *ALPGEN, a generator for hard multiparton processes in hadronic collisions*, *JHEP* **0307** (2003) 001 [[hep-ph/0206293](#)].
- [112] T. Gleisberg, S. Hoeche, F. Krauss, M. Schonherr, S. Schumann *et. al.*, *Event generation with SHERPA 1.1*, *JHEP* **0902** (2009) 007 [[0811.4622](#)].
- [113] J. Alwall, M. Herquet, F. Maltoni, O. Mattelaer and T. Stelzer, *MadGraph 5 : Going Beyond*, *JHEP* **1106** (2011) 128 [[1106.0522](#)].
- [114] G. D’Agostini, *A Multidimensional unfolding method based on Bayes’ theorem*, *Nucl.Instrum.Meth.* **A362** (1995) 487–498.

- [115] A. Hocker and V. Kartvelishvili, *SVD approach to data unfolding*, *Nucl.Instrum.Meth.* **A372** (1996) 469–481 [[hep-ph/9509307](#)].
- [116] V. Blobel, *An Unfolding method for high-energy physics experiments*, [hep-ex/0208022](#).